STUDY OF INTERACTIONS OF DNA WITH RECA AND OTHER PROTEINS

by

Weixian Shi

A dissertation submitted in partial fulfillment
of the requirements for the degree of
Doctor of Philosophy
(Chemical Engineering)
in The University of Michigan
2008

Doctoral Committee:

Professor Ronald G. Larson, Chair
Professor David T. Burke
Assistant Professor Joerg Lahann
Assistant Professor Michael Mayer

This dissertation is dedicated to my dear parents and my wife, Fang.

ACKNOWLEDGMENTS

I would like to take this opportunity to express my sincere thanks for my advisor, Prof. Ronald G. Larson. He has been a great mentor. The discussion with him is always inspiring and leads to the fine thoughts behind the experiment phenomena. His broad knowledge and kind personality have been the driving force for me to move forward throughout my Ph.D. life both academically and personally, which I have enjoyed. I would also give my deep appreciations to my dissertation committee, Prof. David Burke, Prof. Joerg Lahann, and Prof. Michael Mayer. They have given me great advices and academic support.

Larson Group members, both former and current, have been sharing their time to discuss interesting issues with me in addition to the research work. We also played togther and had wonderful times. These activities are indispensable ingredients that make a splendid Ph.D. life. I want to thank you all. They are Hua, Lei, Bruce, Lin, Chih Chen, Jihoon, Tyson, Qiang, Youngsuk, Hwankyu, Susan, Xue, Senthil, Zouwei, Nobu, Semant, Sachin, Anshuman, Laura, Sean.

Special thanks go to Zhiyong, a former postdoc at Kotov' lab, and Haifeng, who have taught valuable knowledge on the usage of AFM. Prof. Kotov and Prof. Burns have allowed me using the equipments in their labs for an extended time. I want to thank them for their generosity. Several friends on central campus, Qian and Wei, have helped me on understanding biological assays, I also want to thank them.

I'd like to thank all departmental staffs, especially Susan Hamlin, Rhonda Sweet, Claire O'Connor, Leslie Cypert, and Mike Africa for their constant help.

Finally, I want to thank my family for supporting me through all these years with their understanding and patience, especially my wife, Fang, who is the greatest part of my life.

TABLE OF CONTENTS

LIST OF FIGURES

Figure

CHAPTER I
INTRODUCTION

Motivation and Background

Manipulation of DNA molecules

DNA molecules have continued to attract enormous research interests. On one hand, the study on DNA molecule itself, as a particular type of polymer that can be imaged optically, provides valuable information on polymer dynamics and mechanics, which helps the understanding of polymer entanglements or the properties of diluted polymer solutions.[1-2] On the other hand, its extreme biological importance as the carrier of genetic information intrigues the extensive investigation of its synthesis, packaging, repair, and other regulatory roles, which usually involves the participation of relevant proteins, such as histone protein, RecA, and DNA/RNA polymerase.[3-5] The manipulation of DNA molecules represents an important step in the in vitro study of protein and DNA interactions since DNA molecules are typically wrapped and entangled in eukaryotic cells, creating a barrier to the clear visualization of the binding sites of protein molecules.[6]

Manipulating DNA molecules can be achieved by attaching one end or both ends of the linear DNA molecule to fixed surfaces, such as treated glass and mica surfaces, or

to small controllable substrates, such as polystyrene beads or sharp tips. The fixed DNA molecules are then made to move, rotate, or extend via either optical traps, magnetic fields, flow fields, or electric fields.[7-10] The manipulation of individual DNA molecule involves two forces, the interfacial force that maintains DNA molecules on the substrate and the manipulating force that contributes to the desired motion of DNA molecules. While the interfacial force could be chemical bonds or hydrophobic interactions, the manipulating force could be viscous forces from the flow, meniscus forces at moving interfaces, magnetic forces, electric forces, or mechanic forces.

A systematic study of stretching of DNA during droplet evaporation has earlier been carried out on a 3-aminopropyltrimethoxysilane (APTES) treated cover glass surface.[11] The study analyzed the motion of linear λ phage DNA (48502 base pairs) near the surface during evaporation by both experiment and simulation. During the evaporation process, part of DNA molecules was attached to the surface via electrostatic interactions, while the viscous force in the flow of the evaporating droplet brought other parts of the molecule to the surface, resulting in stretched DNA molecules near the surface. Faster stretching was achieved by depositing a droplet of DNA solution onto polymer treated surfaces and suctioning it up from the center of droplet [12], yielding a similar alignment as that of drop evaporation. The hydrophobic interaction between the exposed DNA bases and the polymer surface may help fix DNA bases onto the surface, while the meniscus force at the moving droplet-surface-air interface extends DNA molecules along the radial direction of the droplet. Combined with micro-contact printing (μCP), this method was used to stretch DNA on a PDMS surface and then to transfer the patterned DNA to non-treated surfaces.[13] A spin coater can be used to spin a droplet of

DNA solution on a cover slide coated with polymers which also generates radially-aligned patterns of DNA molecules.[14] Alternatively, well patterned 1D and 2D DNA alignments were obtained by blowing a droplet and moving the contact line over $Mg(AC)_2$ treated surfaces.[15] Molecular "combing" is another example of stretching DNA molecules using a meniscus force. Instead of forcing the liquid phase to move, in molecular "combing", a polymer-coated cover slide is dipped into DNA solutions vertically and then pulled out slowly so that a moving interface is created.[6] A schematic drawing of these methods is shown in Figure 1.1.

Both AC [10] and DC [16] fields can be used to derive stretched/combed DNA molecules between electrodes. The alignment of DNA in DC fields requires the modification of one or both ends of DNA molecules so that one or both ends can be attached onto surfaces that hold the DNA molecule to prevent it from traveling to the electrodes and condensing. The use of AC fields can generate combed DNA molecules between electrodes, the mechanism of which is similar to that of gel electrophoresis. Although fixation of either end of DNA molecules to the electrodes is not required under AC fields, it is necessary for the purpose of DNA manipulation.

The elasticity and motion of single DNA molecules have been studied using optical tweezers [7, 17] and magnetic tweezers [8]. The advantage of optical or magnetic tweezers over meniscus forces or an electric field is that the control of a single DNA molecule with tweezers is more precise even though the equipment itself is more complicated and handling of the equipment requires experience. Although the trapping mechanism is different for optical and magnetic tweezers, one or both ends of DNA molecules are immobilized onto small beads in both cases. Usually, the ends of DNA

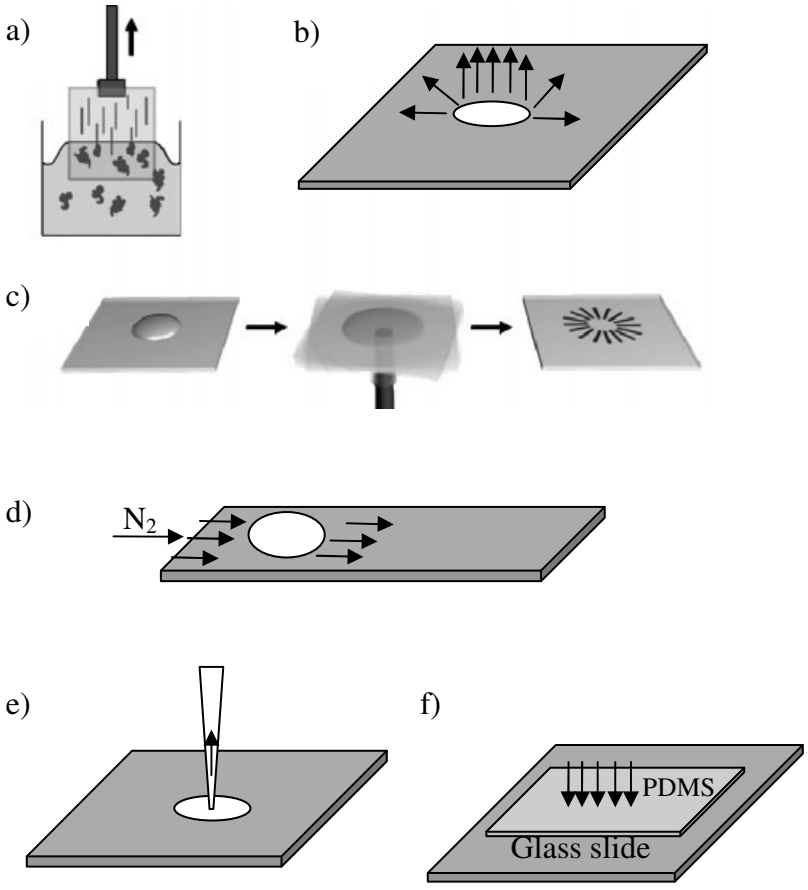

Figure 1.1. Stretching DNA molecules using flows. a) Molecular combing; b) droplet evaporation; c) spin coating; d) blowing; e) suctioning; f) Microcontact printing.

molecules and the beads or surfaces are treated with two pairing reagents, like biotin/streptavidin, respectively.[7] The strong bond between the pairing reagents assists the fixation of DNA molecules. The bead is magnetic for the purpose of manipulation by magnetic tweezers, while there is no special requirement for beads' properties in the case of optical tweezers. The latter uses strongly focused laser beams to hold and move the bead, while magnetic tweezers achieve the same objective by a magnetic field. If the two ends of a single DNA molecule are fixed onto two separate substrates, then stretching and rotating of individual DNA molecules can be achieved by simply moving or spinning the trapped bead.

Direct visualization of protein and DNA interactions

Fluorescence microscopy is a standard experimental technique applied in the study of protein-DNA interactions. Fluorescently labeled DNA molecules are first fixed or stretched before protein solutions are applied, any changes in the DNA molecules or the motion of proteins are imaged. A number of studies have used this method. The cleavage of DNA by various restriction enzymes has been mapped [9, 18] and captured in real-time.[10, 19-20] The processive unwinding and degrading of DNA by RecBCD enzyme, a DNA helicase and nuclease participating in the repair of DNA by recombination, was clearly captured and analyzed with the combination of optical tweezers and fluorescence microscopy.[21] A similar phenomenon was visualized on λ exonuclease digesting λ DNA.[16] The condensation and decondensation of λ DNA induced by protamine were also investigated via fluorescence microscopy.[22] In addition, both protein molecules and DNA molecules were imaged by labeling them with different dyes that emit at different

wavelengths.[19, 23] The use of fluorescently labeled DNA molecules may produce confused results due to possible photocleavage and photobleaching induced by the light source and dye molecules. In fact, the photocleavage of DNA has been observed and analyzed.[24] Although the addition of radical scanvengers may help to quench these disturbing factors to some extent [25], it still might not be advisable to use fluorescence microscopy for long-time observation of DNA samples.

Detailed imaging of protein-DNA interactions can be obtained, both in 2D topographical and in 3D conformational images at nano scales, with scanning probe microscopy (SPM) which is advantageous compared to the submicron resolution and 2D images of fluorescence microscopy. Since the invention of first scanning probe microscope in 1981 by Gerd Binnig and Heinrich Rohrer at the IBM laboratory in Zurich, a series of SPM technologies have emerged. The differences between these SPM techniques are mainly based on the interaction forces between the substances and SPM probes which are used as the detecting signals. Atomic force microscopy (AFM) is one of the most commonly used SPM techniques, which directly detects the topology on surfaces. It can also gather phase information based on the distinct response of different materials on the surface. AFM has become a popular technique for observing biological samples. For example, various DNA molecules have been deposited onto modified mica, glass, or silicon surfaces for observation under AFM or for the production of nano-wires.[12, 14, 26-29]

AFM is also an excellent tool for determining the binding sites of proteins and for capturing the semi-dynamic process of protein-DNA interactions. Yokota et al. have mapped the binding site of GAL4, a transcription factor, on long DNA molecules using

AFM.[30] The association, dissociation, and movement of photolyase (a DNA repair enzyme) over a 500-bp double stranded DNA were visualized under AFM.[31] DNA bending induced by the same enzyme was reported.[32] Other interactions between DNA and repair enzymes were studied using AFM, including Muts protein [33], RecA protein [34], glycosylase [35], Ku protein, DNA-dependent protein keinase, and poly(ADP-ribose) polymerase [36].

RecA protein and its biological functions

RecA protein was first discovered in *Escherichia* coli about 30 years ago.[37] Since then, its analogues have been found in a variety of living organisms, from prokaryotes to eukaryotes.[38-40] Rad51 protein in human body is one of them.[41] It has been proved that RecA-like proteins are involved in various biological functions related to DNA regulations, such as homologous recombination and damaged DNA repair.[37, 42] Although these proteins may possess different peptide sequences, they all function in a similar way.

The main function of RecA-like protein is to catalyze strand exchange interactions.[37, 43] The interaction is composed of three major steps: presynapsis, synapsis, and DNA duplex extension.[44] In the presynapsis step, the RecA protein first covers DNA molecules continuously in a right-handed helix, approximately one RecA monomer per 3 bases or 3 base pairs, and the DNA molecules inside are extended and untwisted.[45] Divalent cations, like Mg^{2+}, are essential for the formation of so-called nucleoprotein filaments. Depend on the other cofactor, either adenosine 5'-triphosphate (ATP), adenosine diphosphate (ADP), or adenosine 5'-(γ-thio) triphosphate (ATPγS), a

nearly non hydrolysable analogue of ATP, the conformation of the nucleoprotein filaments varies. When bound with ATP or ATPyS, the filament shows a pitch around 95nm, while the pitch is only around 65nm when the ADP is bound.[46] The former is called the active or extended form opposed to the compressed or inactive form named for the latter. Only active filaments are biologically active, which are capable of catalyzing strand exchange during which ATP hydrolyzes to ADP.[37] The formation of RecA nucleoprotein filaments on single-stranded DNA (ssDNA) molecules usually requires participation of single-stranded DNA binding (SSB) protein, especially for long ssDNA.[47] SSB removes secondary structures on ssDNA and assists RecA loading. [48] The secondary structures create barriers for RecA binding, and thus preventing the formation of complete and continuous coverage of RecA at these regions. There are two steps during the formation of the nucleoprotein filaments, namely nucleation and extension.[37] The nucleation could occur at multiple locations and the extension grows in the 5' to 3' direction.[49] This directionality of the filament growth remains enigmatic. While both steps are fast on ssDNA, the nucleation step is a slow process on double stranded DNA (dsDNA) molecules and thus is rate-limiting.[37] The presence of a single stranded region, such as a nick, enhances the nucleation step on dsDNA.[50] It is found that stretched dsDNA molecules also appear to have a fast nucleation step.[51]

After the formation of active filaments, the actual strand exchange interaction initiates between an active nucleoprotein filament and a naked dsDNA molecules or the incoming DNA, which is the synapsis step.[44] The initial contact between the filament and the incoming DNA is nonspecific so that both homologous and heterologous DNA can bind to the filament, but only homologous incoming DNA can form stable contact

with the filament after the homology is recognized.[37] At first, there is no interwinding between the filament and the incoming homologous DNA. This type of complex is called a paranemic joint which converts into a plectonemic joint via base pair breaking and reforming. Plectonemic joints are stable even after removal of RecA protein, while paranemic joints require RecA to maintain their structures.[44] More base pairs are broke and reformed during the extension stage coupled with ATP hydrolysis. It is not entirely clear what the role of ATP hydrolysis is during the process since there is no net change of number of base pairs before and after strand exchanges. Because equal numbers of base pairs are broken and reformed, there is no additional energy required. Three-strand exchanges where ATPys were used indicate that strand exchange still proceeds even with little ATP hydrolysis, but with much smaller percentage of completion compared with ATP cases.[52] Additional experiments show that the presence of deficiencies within the incoming dsDNA, such as mismatches, double strand breaks, and nicks inhibit strand exchange if there is no ATP hydrolysis.[53-54] ATP hydrolysis is also required for four-strand exchange.[55] These experiments suggest that ATP hydrolysis may promote the process both kinetically and energetically, i.e., the energy from ATP hydrolysis may be used to speed up the process or conquer the deficiencies which inhibit the strand exchange interactions. The process of strand exchange between a circular ssDNA and a linear dsDNA is shown in Figure 1.2.

While a lot of useful information regarding the functions of RecA has been derived in traditional biochemical assays, single molecular techniques are found to be powerful to reveal more details.[34, 45, 49-51, 56-58] Electron microscopy (EM) is probably the very first single molecular tool that has been used to study the structures of filaments and

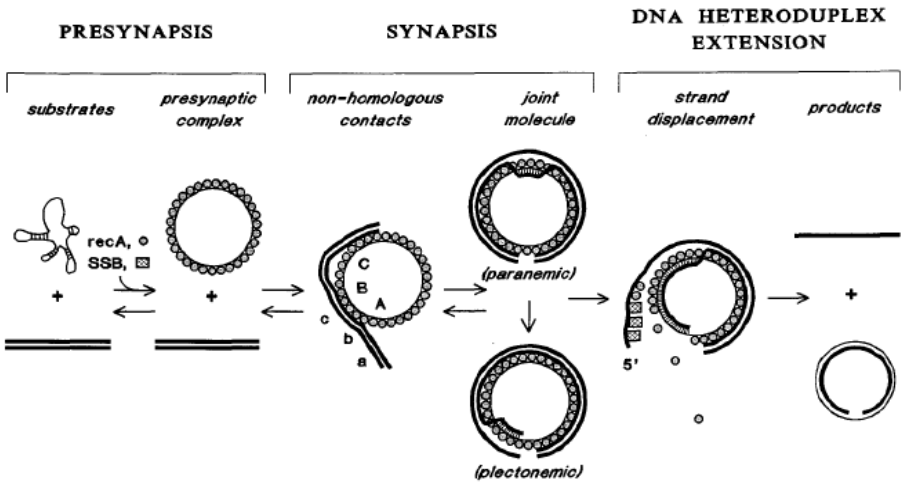

Figure 1.2. RecA-mediated strand exchange interaction. [Adapted from Ref. 37]

strand exchange intermediates.[45] Optical tweezers and magnetic tweezers have been used to study the impact of extensional and rotational forces on the formation of nucleoprotein filaments without labeling either species.[51, 56] Recently, real-time filament formation was seen directly under fluorescence microscopy using optical tweezers.[49] Fast dynamic changes during filament formation were detected using fluorescence resonance energy transfer (FRET). [57] FRET is also capable of monitoring the kinetics during strand exchange processes by selectively labeling two strands with the donor and acceptor dyes.[58] AFM is another tool that have been applied in the study of the semi-dynamics of formation of filaments and impact of SSB on the formation of filaments.[34,50]

Research Objectives (Specific Aims)

Based the accessibility of tools, the goal of this dissertation was set to compare different DNA stretching methods using flow and to understand protein and DNA interactions using both fluorescence microscopy and AFM. To achieve this goal, the following specific aims were defined:

- Evaluation of available methods of stretching DNA molecules using flow fields and determination of appropriate methods that can be used in the study of protein and DNA interactions under fluorescence microscopy.
- Test of the dual-color labeling of protein and DNA molecules and construction of an experimental procedure of dual-color imaging
- Design of an experiment for the study of RecA-filament aggregation behavior

using AFM

- Construction of gel electrophoresis experiments for the understanding of kinetics during strand exchange.

Organization of the Dissertation

The dissertation describes experimental study of protein and DNA interactions. Different DNA stretching techniques are compared and dual-color imaging of protein and DNA interactions is tested in Chapter II. The impact of pH and surfaces on the stretching of DNA molecules is also investigated in this chapter.

Next, the "supercoiled" aggregation of RecA-dsDNA filaments is observed and analyzed using AFM in Chapter III. The handedness and the pitch of "supercoiled" bundles are presented. Chapter IV reports the similar aggregation on RecA-ssDNA filaments and the coiling mechanism is suggested. A kinetic approach regarding RecA-mediated strand exchange is explored in Chapter V. The dual role of ATP hydrolysis and RecA dissociation is connected to experimental observations. Finally, conclusions are drawn and some recommendations for future work are made in Chapter VI.

References

1. Saha, S.; Heuer, D. M.; Archer, L. A., "Electrophoretic mobility of linear and star-branched DNA in semidilute polymer solutions", Electrophoresis 27, 3181-3194 (2006)

2. Hsieh, C. C.; Li, L.; Larson, R. G., "Modeling hydrodynamic interaction in Brownian dynamics: Simulations of extensional and shear flows of dilute solutions of high molecular weight polystyrene", Journal of Rheology 48, 995-1021 (2004)

3. Li, G.; Levitus, M.; Bustamante C.; Widom, J., "Rapid spontaneous accessibility of nucleosomal DNA", Nature Structural & Molecular Biology 12, 46-53 (2005)

4. Bazemore, L. R.; Takahashi M.; Radding C. M., "Kinetic analysis of pairing and strand exchange catalyzed by RecA - Detection by fluorescence energy transfer", Journal of Biological Chemistry 272, 14672-14682 (1997)

5. Xie, S. N., "Single-molecule approach to enzymology", Single Molecules 2, 229-236 (2001)

6. Bensimon, D.; Simon, A. J.; Croquette, V.; Bensimon A., "Stretching DNA with a receding meniscus-experiments and models", Physical Review Letters 74, 4754-4757 (1995)

7. Baumann, C. G.; Bloomfield, V. A.; Smith, S. B.; Bustamante, C.; Wang, M. D.; Block, S. M., "Stretching of single collapsed DNA molecules", Biophysical Journal 78, 1965-1978 (2000)

8. Strick T. R.; Allemand J. F.; Bensimon D.; Bensimon A.; Croquette, V., "The elasticity of a single supercoiled DNA molecule", Science 271, 1835-1937 (1996)

9. Jing, J. P.; Reed, J.; Huang, J.; Hu, X. H.; Clarke, V.; Edington, J.; Housman, D.; Anantharaman, T.; Huff, E. J.; Mishra, B.; Porter, B.; Shenker, A.; Wolfson, E.; Hiort C.; Kantor, R.; Aston, C.; Schwartz, D. C., "Automated high resolution optical mapping using arrayed fluid-fixed DNA molecules", Proceeding of the National Academy of Sciences of The United States of America 95, 8046-8051 (1998)

10. Washizu, M.; Kurosawa, O.; Arai, I.; Suzuki, S.; Shimamoto, N., "Application of eletrostaic stretch-and-positioning of DNA", IEEE Transactions on Industry applications 31, 447-456 (1995)

11. Chopra, M.; Li, L.; Hu, H.; Larson, R. G., "DNA molecular configurations in an evaporating droplet near a glass surface", Journal of Rheology 47, 1111-1132 (2003)

12. Sasou, M.; Sugiyama, S.; Yoshino, T.; Ohtani, T., "Molecular flat mica surface silanized with methyl-trimethoxysilane for fixing and straightening DNA", Langmuir 19, 9845-9849 (2003)

13. Nakao, H.; Gad, M.; Sugiyama, S.; Otobe, K.; Ohtani, T. "Transfer-printing of highly aligned DNA nanowires", Journal of the American Chemical Society 125, 7162-7163 (2003)

14. Ye, J. Y.; Umemura, K.; Ishikawa M.; Kuroda, R., "Atomic force microscopy of DNA molecules stretched by spin-coating technique", Analytical Biochemistry 281, 21-25 (2000)

15. Deng, Z. X.; Mao, C. D., "DNA-templated fabrication of 1D and 2D crossed metallic nanowire arrays", Nano Letters 3, 1545-1548 (2003)

16. Matsuura, S.; Komatsu, J.; Hirano, K.; Yasuda, H.; Takashima, K.; Katsura, S.; Mizuno, A, "Real-time observation of a single DNA digestion by λ exonuclease under a fluorescence microscope field", Nucleic Acids Research 29, e79 (2001)

17. Perkins, T. T.; Smith, D. E.; Chu, S., "Direct observation of tube-like motion of a single polymer chain", Science 264, 819-822 (1994)

18. Cai, W. E.; Jing, J. P.; Irvin, B.; Ohler, L.; Rose, E.; Shuzuya, H.; Kim, U. J.; Simon, M.; Anantharaman, T.; Mishra, B.; Schwartz, D. C., "High-resolution restriction maps of bacterial artificial chromosomes constructed by optical mapping", Proceeding of the National Academy of Sciences of The United States of America 95, 3390-3395 (1998)

19. Kabata, H.; Okada, W.; Washizu, M., "Single-molecule dynamics of the EcoRI enzyme using stretched DNA: its application to in situ sliding assay and optical DNA Mapping", Japanese Journal of Applied Physics 39, 7164-7171 (2000)

20. Schafer, B.; Gemeinhardt, H.; Uhl, V.; Greulich, K. O., "Single molecule DNA Restriction analysis in the light microscope", Single Molecules 1, 33-40 (2000)

21. Bianco, P. R.; Brewer, L. R.; Corzett, M.; Balhorn, R.; Yeh, Y.; Kowalczykowski, S. C.; Baskin, R. J., "Processive translocation and DNA unwinding by individual RecBCD enzyme molecules", Nature 409, 374-378 (2001)

22. Brewer, L. R.; Corzett, M.; Balhorn, R., "Protamine-induced condensation and decondensation of the same DNA molecule", Science 286, 120-123 (1999)

23. Diez, S.; Reuther, C.; Dinu, C.; Seidel, R.; Mertig, M.; Pompe, W.; Howard, J., "Stretching and transporting DNA molecules using motor proteins", Nano Letters 3, 1251-125 (2003)

24. Akerman, B.; Tuite, E., "Single- and double-strand photocleavage of DNA by YO, YOYO and TOTO", Nucleic Acids Research, 24, 1080-1090 (1996)

25. Kanony, C.; Akerman, B.; Tuite, E., "Photobleaching of asymmetric cyanines used for fluorescence imaging of single DNA molecules. Journal of the American Chemical Society 123, 7985-7995 (2001)

26. Lyubchenko, Y. L.; Shlyakhtenko, L. S.; Harrington, R.; Oden, P.; Lindsay, S., "Atomic force microscopy of long DNA: imaging in air and under water", Proceeding of the National Academy of Sciences of The United States of America 93, 2137-2140 (1993)

27. Lyubchenko, Y. L.; Shlyakhtenko L. S., "Visualization of supercoiled DNA with atomic force microscopy in situ", Proceeding of the National Academy of Sciences of The United States of America 94, 496-501 (1997)

28. Pietrement, O.; Pastre, D.; Fusil, S.; Jeusset, J.; David, M. O.; Landousy, F.; Hamon, L.; Zozime, A.; Cam, E. L., "Reversible binding of DNA on $NiCl_2$-treated mica by varying the ionic strength", Langmuir 19, 2536-2539 (2003)

29. Ma, Y. F.; Zhang, J. M.; Zhang, G. J.; He, H. X., "Polyaniline nanowires on Si surfaces fabricated with DNA Templates", Journal of the American Chemical Society 126, 7097-7101 (2004)

30. Yokota, H.; Nickerson, D. A.; Trask, B. J.; van den Engh, G.; Hirst, M.; Sadowski, I.; Aebersold, R., "Mapping a protein-binding site on straightened DNA by atomic force microscopy", Analytical Biochemistry 264, 158-164 (1998)

31. van Noort, S. J. T.; van der Werf, K. O.; Eker A. P. M.; Wyman, C.; de Grooth, B. G.; van Hulst, N. F.; Greve, J., "Direct visualization of dynamic protein-DNA interactions with a dedicated atomic force microscope", Biophysical Journal 74, 2840-2849 (1998)

32. van Noort, J.; Orsini, F.; Eker A.; Wyman, C.; de Grooth, B.; Greve, J., "DNA bending by photolyase in specific and non-specific complexes studied by atomic force microscopy", Nucleic Acids Research 27, 3875-3880 (1999)

33. Sun, H. B.; Yokota, H., "MutS-mediated detection of DNA mismatches using atomic force microscopy", Analytical Chemistry 72, 3138-3141 (2000)

34. Umemura, K.; Komatsu, J.; Uchihashi, T.; Choi, N.; Ikawa, S.; Nishinaka, T.; Shibata, T.; Nakayam, Y.; Katsura, S.; Mizuno, A.; Tokumoto, H.; Ishikawa, M.; Kuroda, R., "Atomic force microscopy of RecA-DNA complexes using a carbon nanotube tip", Biochemical and Biophysical Research Communications 281, 390-395 (2001)

35. Chen, L. W.; Haushalter, K.A.; Lieber, C. M.; Verdine, G. L., "Direct visualization of a DNA glycosylase searching for damage", Chemistry & biology 9, 345-350 (2002)

36. Pang, D.; Vidic, B.; Rodegers, J.; Berman, B. L.; Dritshilo, A., "Atomic force microscope imaging of DNA and DNA repair proteins: applications in radiobiological research", Radiation Oncology Investigations 5, 163-169 (1997)

37. Cox, M. M., "Binding two DNA molecules at once: the RecA protein" in: Revzin A. (eds.), "The biology of nonspecific DNA-protein interactions" CRC Press, Boca Raton, U.S.A, 1990, 171-196

38. van Noort, J.; van der Heijden, T.; de Jager, M.; Wyman, C.; Kanaar, R.; Dekker, C., "The coiled-coil of the human Rad50 DNA repair protein contains specific segments of increased flexibility", Proceeding of the National Academy of Sciences of The United States of America 100, 7581-7586 (2003)

39. Datta, S.; Prabu, M. M.; Vaze, M. B.; Ganesh, N.; Chandra, N. R.; Muniyappa, K.; Vijayan, M., "Crystal structures of Mycobacterium tuberculosis RecA and its complex with ADP-AlF4: implications for decreased ATPase activity and molecular aggregation", Nucleic Acids Research 28, 4964-4973 (2000)

40. Hedayati, M. A.; Steffen, S. E.; Bryant, F. R., "Effect of the Streptococcus pneumoniae MmsA protein on the RecA protein-promoted three-strand exchange reaction - Implications for the mechanism of transformational recombination", Journal of Biological Chemistry 277, 24863-24869 (2002)

41. Gupta, R. C.; Folta-Stogniew, E.; O'Malley, S.; Takahashi, M.; Radding, C. M., " Rapid exchange of A : T base pairs is essential for recognition of DNA homology by human Rad51 recombination protein", Molecular Cell 4, 705-714 (1999)

42. West, S. C., "Molecular views of recombination proteins and their control", Nature Reviews Molecular Cell Biology 4, 435-445 (2003)

43. Bianco, P. R.; Tracy, R. B.; Kowalzcykowski, S. C., "DNA strand exchange proteins: a biochemical and physical comparison", Frontiers in Bioscience 3, d570-603 (1998)

44. Kowalzcykowski, S. C.; Egglestson, A. K., "Homologous paring and DNA paring and DNA strand-exchange proteins", Annual Review of Biochemistry 63, 991-1043 (1994)

45. Egelman, E. H.; Stasiak, A., " Structure of helical RecA-DNA complexes: complexes formed in the presence of ATP-Gamma-S or ATP", Journal of Molecular Biology 191, 677-697 (1986)

46. Yu, X.; Egelman, E. H.., "Structural data suggest that the active and inactive forms of the RecA filament are not simply interconvertible", Journal of Molecular Biology 227, 334-346 (1992)

47. Kowalczykowski, S. C.; Krupp, R. A., "Effects of Escherichia coli SSB protein on the single-stranded DNA-dependent ATPase activity of Escherichia coli RecA protein-evidence that SSB protein facilitates the binding of RecA protein to regions of secondary structure within single-stranded DNA", Journal of Molecular Biology 193, 97-113 (1987).

48. Muniyappa, K.; Williams, K.; Chase, J. W.; Radding, C. M., "Active nucleoprotein filaments of single-stranded binding protein and RecA protein on single-stranded DNA have a regular repeating structure", Nucleic Acids Research 18, 3967-3973 (1990)

49. Galletto, R.; Amitani, I.; Baskin, R. J.; Kowalczykowski, S. C., " Direct observation of individual RecA filaments assembling on single DNA molecules", Nature 443, 875-878 (2006)

50. Sattin, B. D.; Goh, M. C., "Direct observation of the assembly of RecA/DNA complexes by atomic force microscopy", Biophysical. Journal 87, 3430-3436 (2004)

51. Hegner, M.; Smith, S. B.; Bustamante, C., "Polymerization and mechanical properties of single RecA-DNA filaments", Proceeding of the National Academy of Sciences of The United States of America 96, 10109-10114 (1999)

52. Shan, Q.; Cox, M. M.; Inman, R. B., "DNA strand exchange promoted by RecA K72R - two reaction phases with different Mg2+ requirements", Journal of Biological Chemistry 271, 5712-5724 (1996)

53. Bianchi, M.; Radding, C. M., " Insertions, deletions and mismatches in heteroduplex DNA made by RecA protein", Cell 35, 511-520 (1983)

54. Shan, Q.; Cox, M. M., "On the mechanism of RecA-mediated repair of double-strand breaks: No role for four-strand DNA pairing intermediates", Molecular Cell 1, 309-317 (1998)

55. Kim, J. I.; Cox, M. M.; Inman, R. B., "On the role of ATP hydrolysis in RecA protein-mediated DNA strand exchange II. Four-strand exchanges", Journal of Biological Chemistry 267, 16444-16449 (1992)

56. van der Heijden, T.; van Noort, J.; van Leest, H.; Kanaar, R.; Wyman, C.; Dekker, N.; Dekker, C., "Torque-limited RecA polymerization on dsDNA", Nucleic Acids Research 33, 2099-2105 (2005)

57. Joo, C.; McKinney, S. A.; Nakamura, M.; Rasnik, I.; Myong, S.; Ha, T., "Real-time observation of RecA filament dynamics with single monomer resolution", Cell 126, 515-527 (2006)

58. Bazemore, L. R.; Takahashi, M.; Radding, C. M., "Kinetic analysis of pairing and strand exchange catalyzed by RecA - detection by fluorescence energy transfer", Journal of Biological Chemistry 272, 14672-14682 (1997)

CHAPTER II
STRETCH OF DNA MOLECULES USING FLOWS AND VISUALIZATION OF PROTEIN AND DNA INTERACTIONS UNDER FLUORESCENCE MICROSCOPY

Chapter Summary

DNA molecules were stretched by evaporation, suctioning, or blowing of a DNA-containing water droplet on polydimethylsiloxane (PDMS) sheets, polystyrene (PS) or poly methyl-methacrylate (PMMA) coated cover slides. While the bulk flow during droplet evaporation can by itself stretch DNA, a water-air meniscus moving along a surface to which part of a DNA molecule is adsorbed can exert stronger forces on the DNA molecule, and therefore play the dominant role in the stretching of DNA molecules by suctioning or blowing, resulting in longer extension of DNA molecules. The irregular motion of the moving droplet captures under a high speed camera indicates that the flow involved is complicated during the blowing process. The change of hydrophobic interaction due to the change of pH or surfaces is likely not the sole reason leading to the different behaviors of DNA molecules upon stretched by blowing methods, the detailed structure of individual polymers on the surface might also affect the interaction between DNA molecules and the surfaces. The motion of TRITC-labeled DNAse I molecules in the vicinity of YoYo-1-lableled DNA molecules stretched on surfaces shows possible nonspecific interactions captured by the dual-color imaging system.

Introduction

The study of protein-DNA interactions is crucial for the better understanding of biological processes such as DNA replication, repair, recombination, and other cellular processes.[1-4] Direct visualization of these interactions *in vitro* usually requires unwrapping and stretching of DNA molecules which are tightly and intricately packaged in the nucleus in the multi-scale structures of chromatin. [1, 4-6]

Methods for stretching and manipulating single DNA molecules are developed during past decades, including use of flows [7-9], electric fields [10-12], magnetic[13] and optical tweezers [14-15]. Of those methods, stretching of DNA molecules using flow fields is probably the most convenient because it does not rely on complex tools like optical or magnetic tweezers or intense and high frequency electric or magnetic fields. There are two types of stretching forces exerted on DNA molecules in flows near surfaces, namely viscous drag forces produced by the bulk flows [9] and meniscus forces generated by the motion of an air-water interface along a DNA molecule [16-17]. In both cases, the stretching is more effective when part of the molecule is pinned to a surface by electrostatic interactions [9, 18], hydrogen bonds [19], or covalent bonds [11]. For example, APTES [8-9] or magnesium [18] treated surfaces (positively charged) can absorb negatively charged DNA molecules by ionic interactions. DNA can be stretched by evaporating a droplet [8], blowing the droplet with air [18], or by spin coating DNA solution [20] on such surfaces. Hydrophobic surfaces such as PDMS or PMMA can also be used to bind DNA, where the adhesion force is mostly hydrophobic interactions between locally unpaired bases and hydrophobic surfaces. The unpaired bases can be prevalent at the ends of the DNA chain at acidic pHs. Suctioning of a droplet on PDMS by a pipette can also

generate flows that stretch DNA molecules.[21] The stretched DNA molecules were subsequently transferred to non-treated cover glass or mica surfaces through microcontact printing (μCP) and visualized by fluorescence microscopy or AFM. DNA can also be stretched when a hydrophobic surface is slowly pulled out of a DNA-containing solution.[22] This so-called "molecular combing" technique also uses a moving interface to stretch and align DNA molecules.

Given the development of multiple methods of stretching DNA, it would be desirable to compare them systematically to determine which stretches most effectively and consistently, and with greatest convenience. While only suctioning, blowing, and evaporation methods were used and discussed in this study, two other methods (molecular combing and spin coating) were also studied by the other group member. The combined results were published in 2007 [23] and part of this chapter is adapted from the published paper.

Materials and Methods

Materials

λ DNA (500ug/mL, 48.5k bps, New England Biolabs), 10 mM Tris-HCl 1mM EDTA (TE) buffer (pH 8.0), 50 mM MES buffer (pH 5.5), 50 mM Bbis-Tris buffer (pH 6.6), YoYo-1(1mM, Invitrogen), Silicon Elastomer (Dow Corning), APTES(Sigma). DNAse I (powder, Sigma), tetramethylrhodamine-isothiocyanate (TRITC, Invitrogen), Dimethylformamide (DMF, Pierce), phosphate buffer saline (PBS, Sigma). DNA was labeled by YoYo-1 dye at ratios of 1 dye molecule per 5 or 8 base pairs and diluted with buffers at desired pH values. DNAse I (10mg/mL in PBS) was mixed with TRITC

(10mg/mL in DMF) at a molar ratio of 1:8 for 1hr at 25 ^{O}C and the mixture was filtered through a gel column packed with sephadex G25 gel (Pierce) to get rid of free dye molecules.

Droplet evaporation

Evaporative stretching was conducted on APTES-treated glass surfaces as described in our previous work [9]. Briefly, glass surfaces were cleaned in boiling concentrated nitric acid and hydrochloric acid followed by deionized water rinsing and then treated with 100 ppm of 2% (volume) APTES water solution in ethanol in a glove box with nitrogen blowing in. DNA was diluted to 20~50pg/μl and YoYo-1 was loaded at a ratio of 1:8. Then a 0.25~1.0 μl droplet was deposited onto an APTES-treated cover glass which has been aged for 1~7 days before deposition, and images were taken during and after evaporation.

Suctioning

DNA was diluted to 500pg/μl with a YoYo-1 loading of 1:5. PDMS sheets were prepared with overnight healing. A 5ul to 40 μl droplet was deposited onto the surface and suctioned up after around 20 seconds. Then, the PDMS sheet was pushed gently against a cover glass for imaging with fluorescence microscopy.

Blowing

DNA was diluted to 50~ 5000 pg/μl with a YoYo-1 loading of 1:5. A 15 μl to 30 μl of DNA solution was deposited onto a PDMS sheet and forced to move by blowing

nitrogen gas at the bottom of the droplet. Then the sheet was cut into small pieces. These PDMS pieces with DNA patterns were then pushed against cover slides and imaged.

Microcontact printing

To transfer and fix DNA that are stretched on PDMS slabs onto a cover glass, an appropriate pressure was engaged onto small PDMS pieces (~5mm×5mm) followed by pealing off the PDMS piece from the cover glass. Pre-treatment of the cover glass is not necessary.

Visualization of DNAse I and DNA interactions

After DNA being stretched, solution of DNAase I was introduced onto cover slides via a small channel made of PDMS. The hydraulic force drives the protein solution entering from one end of the channel and exiting from the other end. The imaging system was programmed to alternate between the blue excitation (488nm) and green excitation (536nm) so that DNA images and protein images were captured in turn. The frequency of capture is approximately one frame per second. Two neighboring images were merged together using Matlab and movie clips were generated using Adobe Premier.

Results and Discussion

Droplet evaporation

Most of the DNA molecules stretched on the surface via evaporation show a length less than 16μm, the contour length of non-stained DNA. The average length of

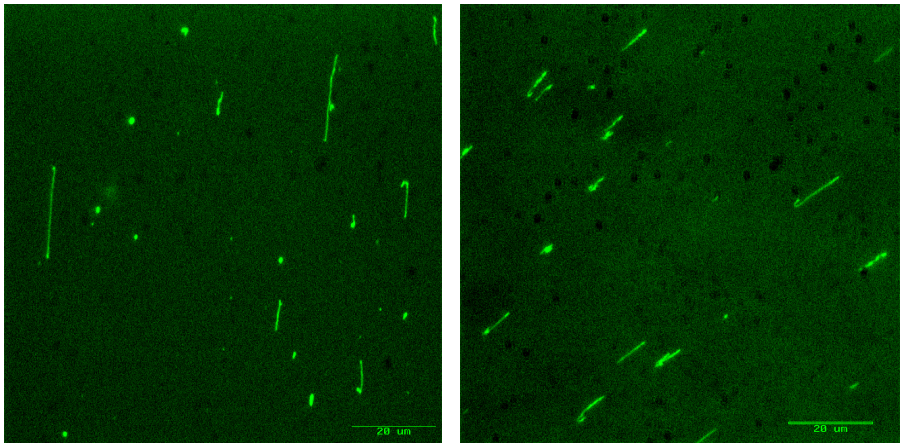

Figure 2.1. λ DNA (Dye:bps = 1:8) stretched on APTES-coated glass surfaces via droplet evaporation. Left: DNA stretched with a droplet of 0.25 µl at 40pg/µL; Right: DNA stretched with a droplet of 0.4µl at 40pg/µL. The scale bar is 20µm.

DNA is 4.11 μm, which is consistent with our group's previous work [9]. The surface coverage of DNA molecules depends on the location of the imaging area within the original droplet, which is also a factor that contributes to the extent of stretch. There is one problem with this method: the reproducibility of obtaining the patterned DNA shown in Figure 2.1 is less than desirable. That is DNA might not be stretched in some cases due to poor ATPTES treatment. Additionally, the speed of evaporation is not stable in all cases due to the fluctuation of the humidity of atmosphere, of the airflow surrounding the droplet, and of the method of deposition of the droplet onto the surface.

Suctioning

μCP is reported to yield well-patterned DNA molecules on glass surfaces without any treatment [21]. Figure 2.2 (a) shows both the DNA patterns obtained by suctioning on PDMS surfaces and those then transferred to glass cover slides. As seen in the image, the direction of alignment is roughly radial, similar to that from droplet evaporation. Furthermore, lengths of stretched DNA molecules are nearly uniform with a commonly seen value of ~22.5μm in selected areas. The patterning is quite repeatable regardless of size of droplet (from 5 μL to 40 μL). The central region of the droplet is not well patterned due to the high concentration of DNA solution left at the final stage of suctioning. This can be clearly seen in the comparison of images at different locations within a 40-μL droplet as shown in Figure 2.2 (b).

Blowing

By blowing a droplet of DNA along one direction on a magnesium-ion-treated

a)

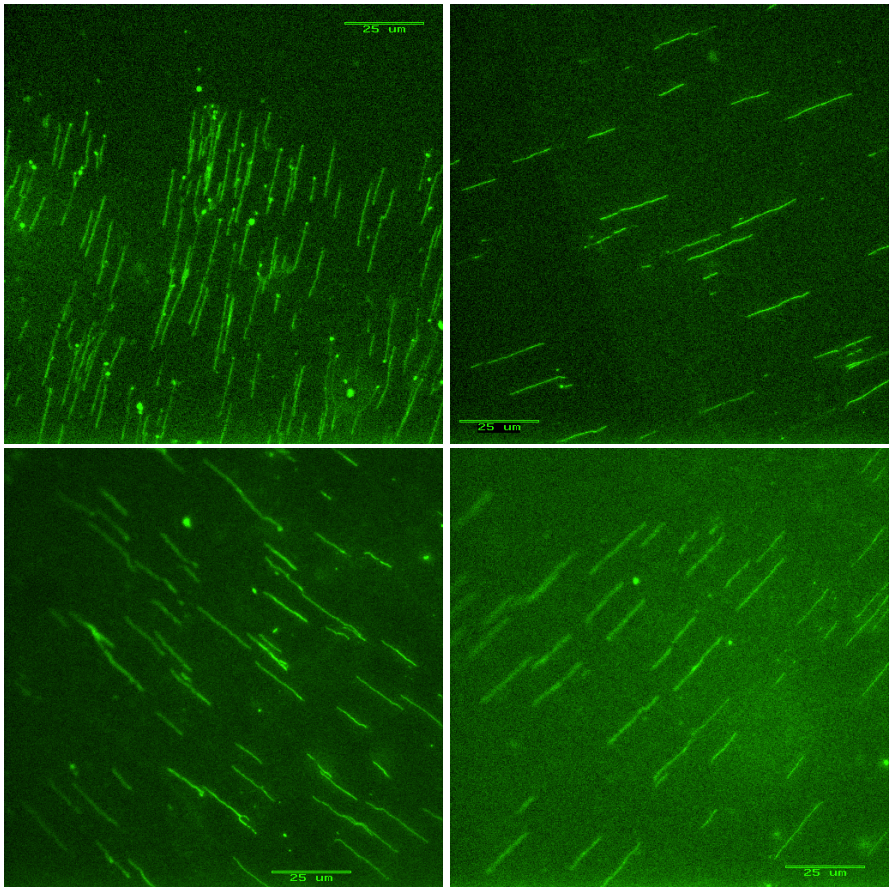

b)

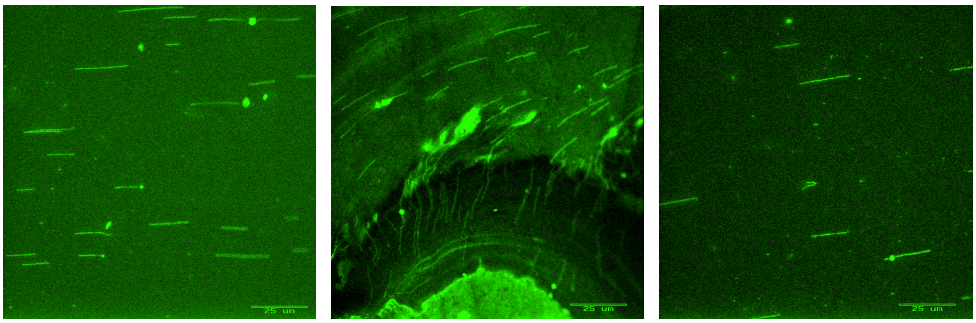

(-1600μm, 200μm) (0, 0) (2000μm, 0)

Figure 2.2. Patterned λ DNA (500pg/ μL, Dye: bps=1:5) using the suctioning method and μCP. (a) DNA stretched on PDMS (top two) with a 5-μL droplet and transferred onto cover glasses (bottom two); (b) stretching patterns at different locations within the initial deposition of a 40-μL droplet. Numbers in parentheses are the coordinates relative to the center of the droplet.

surface, single direction and 2-direction alignments of DNA molecules were obtained.[18] This uniform alignment might make it convenient to study motions of proteins near multiple DNA molecules in a single run. Inspired by these results and our results using suction method plus μCP, we used the blowing method on a PDMS surface and were able to transfer the patterned DNA onto a non-treated cover glass. Although there is an edge effect near the edges perpendicular to the direction of droplet motion, the overall stretching is also quite uniform as can be seen in Figure 2.3 (a). Interestingly, a 2-D network of DNA molecules can be generated at the crossing region by blowing one droplet in one direction followed by a second droplet deposited and blown in a second direction (perpendicular to the first direction, Figure 2.3 (b)). In these images, there is distortion of DNA molecules aligned in the first direction due to the blowing of a droplet along the second direction. This 2-D DNA network may help in the localization of protein molecules for the study of protein-DNA interactions.

Impact of pH and surfaces on the stretching of DNA molecules

We have also extended our study of stretching of DNA molecules at different pHs and on different surfaces using the blowing method to understand the mechanism of stretching. Surfaces used include PMMA, PS, and PDMS, while pH is changed between 5.5 and 8.0. Some simple parameters are defined for the comparison of the DNA stretching. The stretch ratio is simply defined as the stretch length divided by the contour length (L) and the mean value of the stretch ratio is number averaged stretch length (L_n) divided by the contour length. We also define the relative standard deviation (RSTD) as the standard deviation divided by the number averaged stretch length, and similarly the

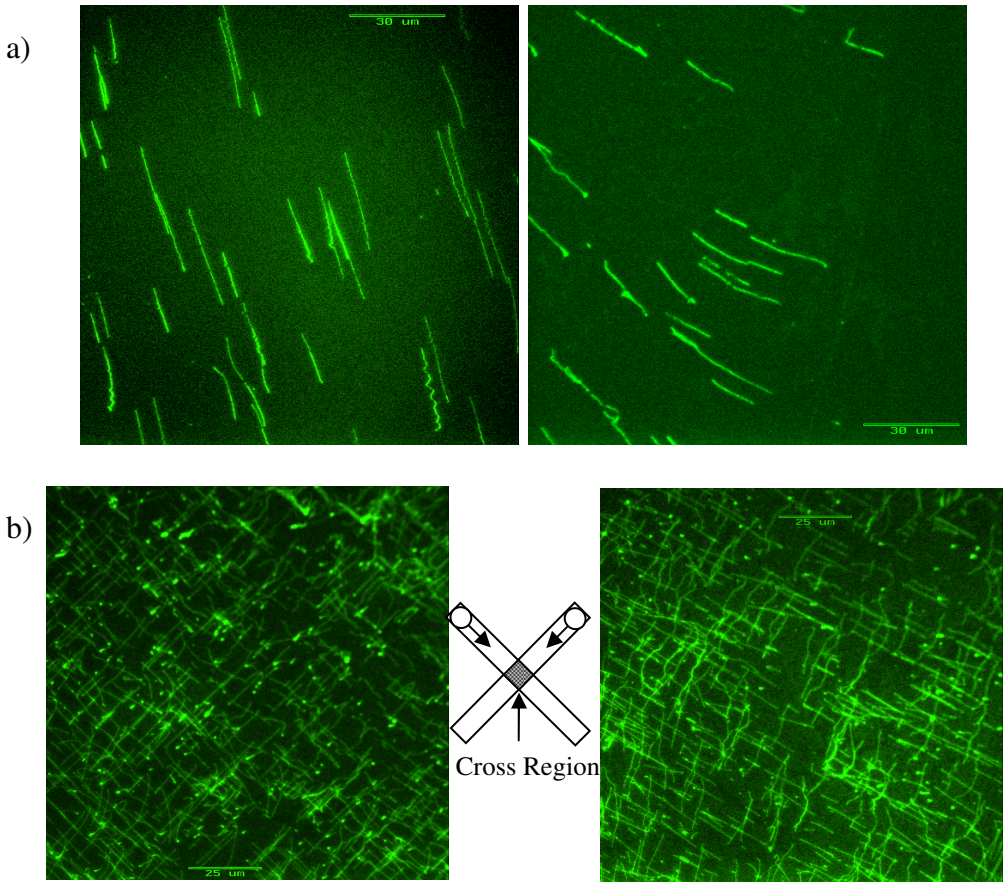

Figure 2.3. Stretching of λ DNA (5ng/μL, Dye:bps=1:5) on PDMS via blowing and transferred onto cover glasses using μCP. (a) 1-D stretching; (b) 2-D stretching.

relative standard error (RSTE) as the standard error divided by the number averaged stretch length.

$$L_n = \frac{\sum_i n_i L_i}{\sum_i n_i} \quad (1)$$

$$RSTD = \frac{STD}{L_n} \quad (2)$$

$$RSTE = \frac{STE}{L_n} \quad (3)$$

Intercalating dye YOYO-1 is known to increase the contour length of the DNA.[24] We assume that the contour length linearly increases with a base pair per dye ratio. When the upper limit of 0.34 nm rise per base pair is used to calculate the contour length of unstained lambda phage DNA, base pair per dye ratios of 8:1 and 5:1 staining will increase the contour length to 18.8μm and 20.1μm, respectively. Typical distributions of stretched DNA molecules at pH 8.0 are shown in Figure 2.4, from top to bottom, PMMA, PS, and PDMS, respectively. The insets are experimental results at pH 6.6. While the pH seems to have little impact on the stretching of DNA molecules on both PMMA and PDMS surfaces, the stretching of DNA molecules on PS surfaces exhibits a strong dependency on pH with the poorest stretching at pH 6.6 as shown in Figure 2.5 (a). The stretching on PS surfaces done at more pH values confirms the tendency (Figure 2.5 (b)). Stronger hydrophobic interactions, occurring at lower pH values or more hydrophobic surfaces, might lead to multiple contact points between DNA molecules and the surface and thus decrease the stretch ratio.[24] But the existence of poorest stretching in the middle of pH range tested in this study can not be explained solely by the change of hydrophobic interactions. Apparently, there are other factors

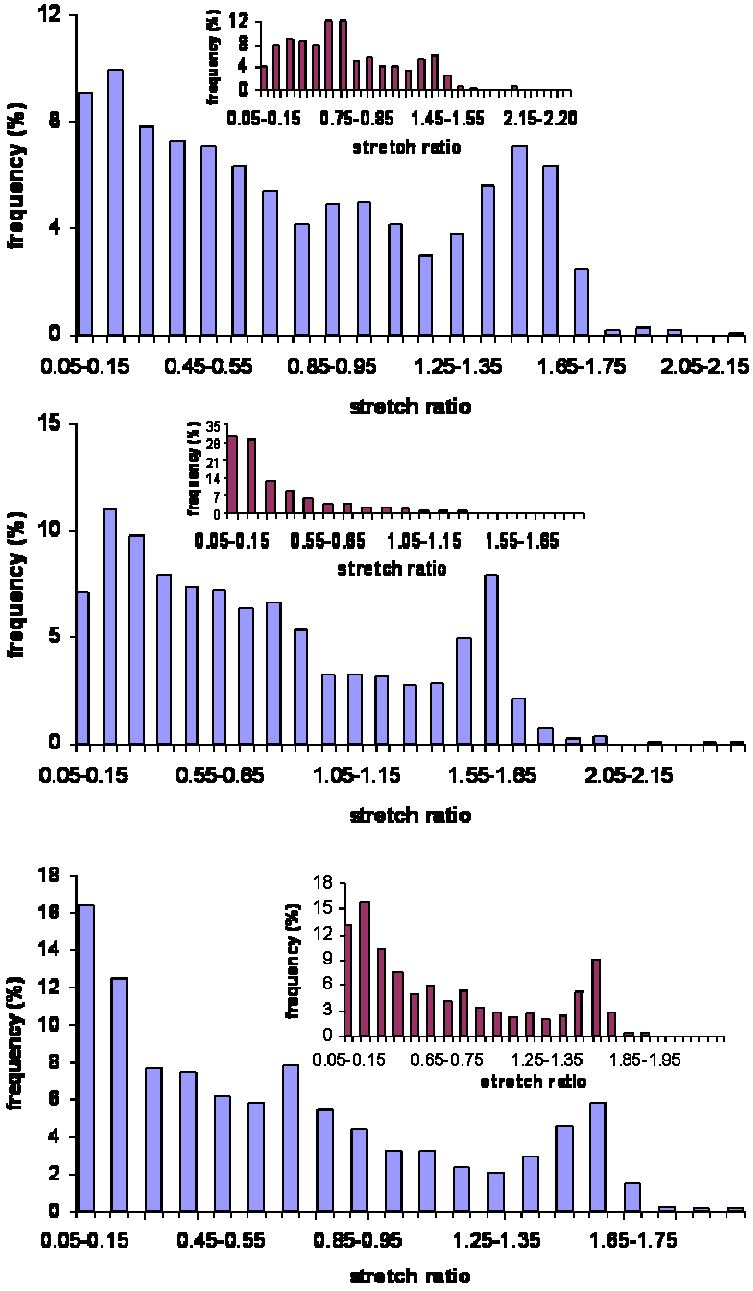

Figure 2.4. Distribution of stretched λ DNA (Dye:bps=1:5) on PMMA (500pg/ μL), PS (50pg/ μL), and PDMS (50pg/ μL) via the blowing method. The large images and the insets were distributions at pH 8.0 and pH 6.6, respectively.

which complicate the effect of pH or surfaces on DNA stretching. It could be the detailed interaction of DNA molecules with function groups on the surface or electrostatic interactions if there is any. The complexity is also reflected on the amount of DNA molecules absorbed onto the surfaces. The statistics shows that DNA molecules have stronger absorption on the surface at lower pH values, consistent with the stronger hydrophobic interaction at acidic conditions, but the different hydrophobic surfaces used actually exhibit irregular impact on the number of DNA molecules absorbed on the surfaces as seen in Figure 2.5 (c). The least hydrophobic PMMA surfaces adsorbs much less DNA molecules even if the concentration is 10-folder higher than that used for PS and PDMS surfaces, but the most hydrophobic PDMS surfaces does not absorb more DNA molecules than the less hydrophobic PS surfaces. Instead, it is the PS surface that is most attractive to DNA molecules.

Other than pH and surface properties, the blowing itself can also generate complexity during the process. A complicated flow pattern has been revealed using a high speed camera. The series of images captured at a speed of 1000 frames/second show that there is serious deformation of the droplet when it is blown (Figure 2.6). The deformed droplet travels on the surface and change its shape regularly that is invisible with bare eyes.

Visualization of DNAse I and DNA interactions

We have successfully imaged both lambda DNA and DNAse I molecules almost synchronously on a fluorescent microscope equipped with a dual-view filter. These two types of molecules were labeled with YoYo-1 (green, excited at 488nm) and TRITC

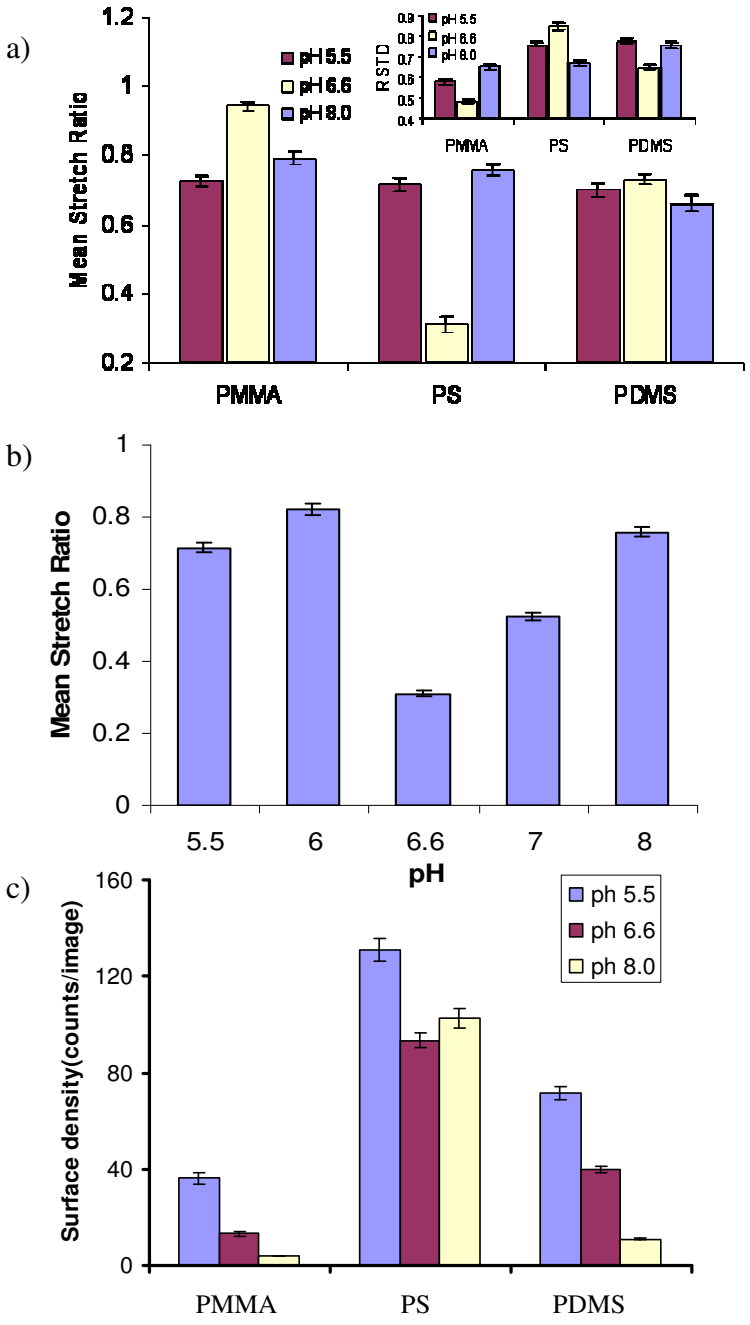

Figure 2.5. Impact of pH on the stretch of λ DNA (Dye:bps=1:5) on PMMA ((500pg/ μL), PS (50pg/ μL), and PDMS (50pg/ μL) via blowing method. (a) The mean stretch ratio is affected both by pH and surfaces; the inset shows the impact on RSTD; (b) Impact of pH on DNA stretching on PS surfaces at additional pH values; (c) The impact of surfaces and pH on the absorption of DNA molecules to the surface.

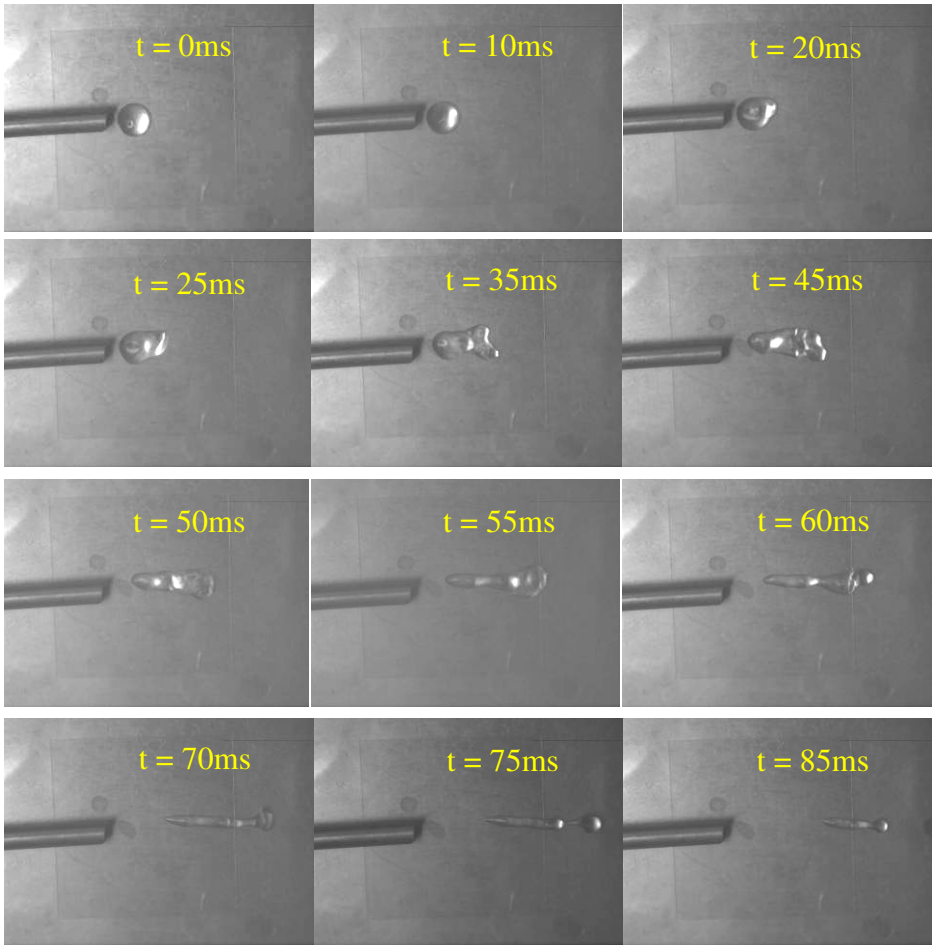

Figure 2.6. The deformation of a droplet during blowing captured at 1000 frames/second.

(orange, excited at 544nm) respectively. A series of images given in Figure 2.7 by superimposing every two connecting frames captured real-time show a DNAse I (the red spot) molecule approaching a lambda phage DNA molecule (the green line), pausing near one end of the DNA and leaving from the DNA. The rates of movement of DNAse I molecule in these 3 stages are much different. It takes the molecule about 10s to find the DNA, during which it traveled about 14.4um and the average velocity is about 1.4μm/s. The velocity decreased to 0.6μm/s once the protein molecule started to move away from the DNA, which is correspondent to a travel distance of 7.5μm in 12.437s. In contrast, the mobility of the protein decreases more sharply during the period when it was pausing or "dancing" around one end of the DNA. It seems that the protein is "caged" during this period. The distance it traveled is only about 5μm in 14.431s, a velocity of 0.27μm/s. Figure 2.8 clearly shows this variation. The results indicate that the DNAse I molecule possibly has an interaction with the DNA molecule via electrostatic interactions. This interaction slowed the protein molecule in the vicinity of DNA and resulted in the slower motion of the protein molecules.

There are several possible problems that have been identified which might prevent us from understanding the interaction. First, YoYo-1 labeled DNA molecules are prone to photobleach or be cleaved under the strong light. Second, the label protein molecules we saw could be in aggregated forms as found by other group member. The aggregation may be caused by the labeling procedure. Furthermore, the interaction that is supposedly to see is designed to occur near or on surfaces which could act as a barrier for protein molecules to access their binding sites on DNA molecules.

Conclusions

The stretching of λ DNA molecules labeled with YoYo-1 has been investigated using fluorescence microscopy. Among the three flowing methods, suctioning and blowing stretch DNA molecules more than the droplet evaporation method. The impact of pH and surfaces were also studied with the blowing method, which reveals that the interfacial force between DNA molecules and the surface results from multiple sources, which complicates the stretching process. Stretched DNA molecules have been successfully applied in the study of DNAse I and DNA interaction under a dual-view imaging system. The characteristic motion of DNAse I molecules were captured and analyzed, showing the "caging" effect when the two molecules get close to each other due to the electrostatic interaction.

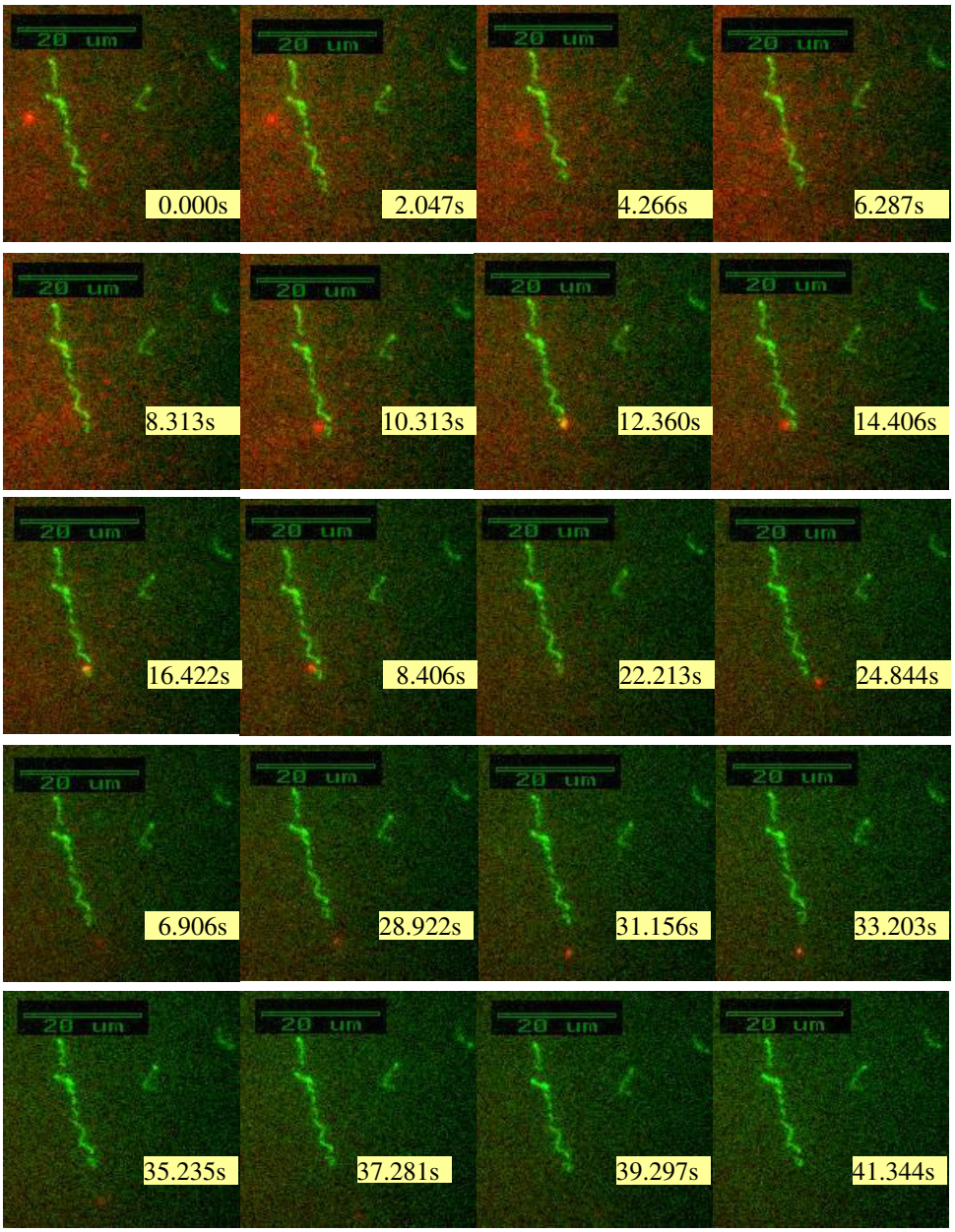

Figure 2.7. The motion of TRITC-labeled DNAse I near a stretched DNA molecule captured with a dual-color imaging system. DNAse I: red dots; DNA: green lines.

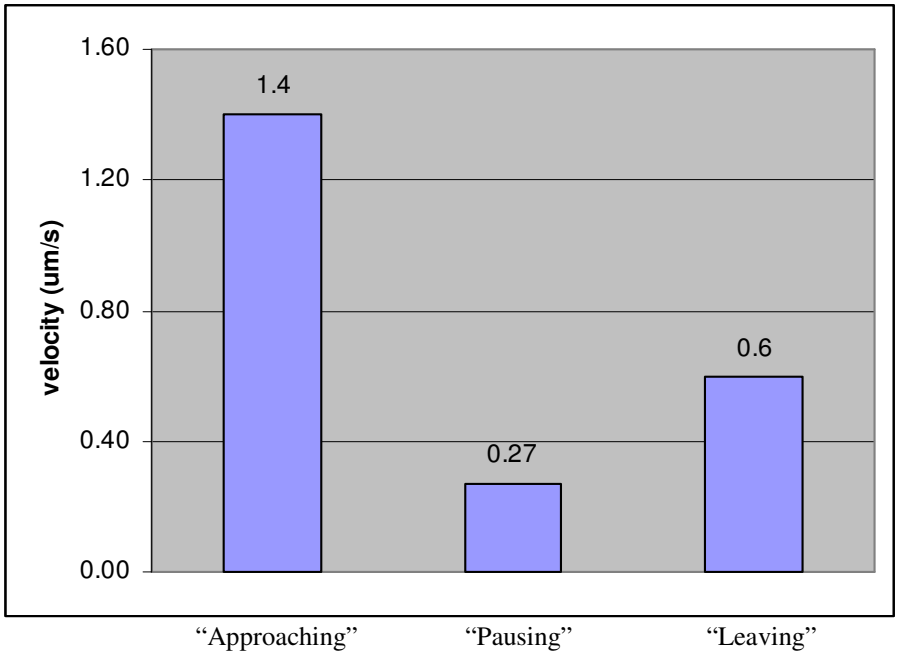

Figure 2.8. The averaged speed of DNAase I in the three distinct stages during the interaction between the protein and the DNA molecule.

References

1. Bianco, P. R.; Brewer, L. R.; Corzett, M.; Balhorn, R.; Yeh, Y.; Kowalczykowski, S. C.; Baskin, R. J., "Processive translocation and DNA unwinding by individual RecBCD enzyme molecules", Nature 409,374-377 (2001)

2. Shav-Tal, Y.; Darzacq, X.; Shenoy, S. M.; Fusco, D.; Janicki, S. M.; Spector, D. L.; Singer, R. H., "Dynamics of single mRNPs in nuclei of living cells", Science 304, 1797-1800 (2004)

3. Friedberg, E. C., "DNA damage and repair", Nature 421, 436-440 (2003)

4. Sun, H. B.; Yokota, H., "MusS-mediated detection of DNA mismatches using atomic force microscopy", Analytical Chemistry 72, 3138-3141 (2000)

5. Koch, S. J.; Shundrovsky, A.; Jantzen, B. C.; Wang, M. D., "Probing protein-DNA interactions by unzipping a single DNA double helix", Biophysical Journal 83, 1098-1105 (2002)

6. Brewer, L. R.; Corett, M.; Balhorn, R., "Protamin-induced condensation and decondensation of the same DNA molecules", Science 286, 120-123 (1999)

7. Haber, C.; Wirtz, D., "Shear-induced assembly of λ-Phage DNA", Biophysical Journal 79, 1530-1536 (2000)

8. Jing, J. P.; Reed, J.; Huang, J.; Hu, X. H.; Clarke, V.; Edington, J.; Housman, D.; Anantharaman, T.; Huff, E. J.; Mishra, B.; Porter, B.; Shenker, A.; Wolfson, E.; Hiort, C.; Kantor, R.; Aston, C.; Schwartz, D.C., "Automated high resolution optical mapping using arrayed fluid-fixed DNA molecules", Proceeding of the National Academy of Sciences of The United States of America 95, 8046-8051(1998)

9. Chopra, M.; Li, L.; Hu, H.; Larson, R. G., "DNA molecular configurations in an evaporating droplet near a glass surface", Journal of Rheology 47, 1111-1132 (2003)

10. Kabata, H.; Kurosawa, O.; Arai, I.; Washizu, M.; Margarson, S. A.; Glass, R. E.; Shimamoto, N., "Visualization of single molecules of RNA Polymerase Sliding along DNA", Science 263, 1561-1563 (1993)

11. Washizu, M.; Kurosawa, O.; Arai, I.; Suzuki, S.; Shimamoto, N., "Application of eletrostaic stretch-and-positioning of DNA", IEEE Transactions on Industry applications 31, 447-456 (1995)

12. Yamamoto, T.; Kurosawa, O.; Kabata, H.; Shimamoto, N.; Washizu, M., "Molecular surgery of DNA based on electrostatic micromanipulation", IEEE Transactions on Industry applications 3, 1010-1017 (2000)

13. Strick T. R.; Allemand J. F.; Bensimon D.; Bensimon A.; Croquette, V., "The elasticity of a single supercoiled DNA molecule", Science 271, 1835-1937 (1996)

14. Baumann, C. G.; Bloomfield, V. A.; Smith, S. B.; Bustamante, C.; Wang, M. D.; Block, S. M., "Stretching of single collapsed DNA molecules", Biophysical Journal 78, 1965-1978 (2000)

15. Perkins, T. T.; Smith, D. E.; Chu, S., "Direct observation of tube-like motion of a single polymer chain", Science 264, 819-822 (1994)

16. Bensimon, A.; Simon, A.; Chiffaudel, A.; Croquette, V.; Heslot, F.; Bensimon, D., "Alignment and sensitive detection of DNA by a moving interface", Science 265 2096-2097(1994)

17. Bensimon, D.; Simon, A. J.; Croquette, V.; Bensimon A., "Stretching DNA with a receding meniscus-experiments and models", Physical Review Letters 74, 4754-4757 (1995)

18. Deng, Z. X.; Mao, C. D., "DNA-templated fabrication of 1D and 2D crossed metallic nanowire arrays", Nano Letters 3, 1545-1548 (2003)

19. Nakao, H.; Hayashi, H.; Yoshino, T.; Sugiyama, S.; Otobe, K.; Ohtani, T., "Development of novel polymer-coated substrates for straightening and fixing DNA", Nano Letters 2, 475-479 (2002)

20. Ye, J. Y.; Umemura, K.; Ishikawa M.; Kuroda, R., "Atomic force microscopy of DNA molecules stretched by spin-coating technique", Analytical Biochemistry 281, 21-25 (2000)

21. Nakao, H.; Gad, M.; Sugiyama, S.; Otobe, K.; Ohtani, T. "Transfer-printing of highly aligned DNA nanowires", Journal of the American Chemical Society 125, 7162-7163 (2003)

22. Gueroui, Z.; Place, C.; Freyssingeas, E.; Berge, B., "Observation by fluorescence microscopy of transcription on single combed DNA", Proceeding of the National Academy of Sciences of The United States of America 99, 6005-6010 (2002)

23. Kim, J. H.; Shi, W. X.; Larson, R. G., "Methods of stretching DNA molecules using flow fields", Langmuir 23, 755-764 (2007)

24. Perkins, T.T.; Smith, D. E.; Larson, R. G.; Chu, S., "Stretching of a single tethered polymer in a uniform flow", Science 268, 83-87 (1995)

CHAPTER III
ATOMIC FORCE MICROSCOPIC STUDY OF AGGREGATION OF RECA-DNA NUCLEOPROTEIN FILAMENTS INTO LEFT-HANDED "SUPERCOILED" BUNDLES

Chapter Summary

RecA and its complexes with double stranded DNA (dsDNA) and single stranded DNA (ssDNA) are responsible for homologous recombination and DNA repair. In this study, we have observed, by atomic force microscopy (AFM), 2-filament left-handed "superhelices" of RecA-dsDNA filaments that further interwind into 4- or 6-filament bundles, in addition to previously reported left-handed bundles of 3 or 6 filaments. Since this type of aggregated bundles was referred as "supercoiled", the same terminology is used in our study while we understand the term is usually specific to circular dsDNA molecules under torsional stresses. Also revealed are 4-filament bundles formed by further interwinding of two intra-filament "superhelices" of individual filaments. Pitches of "superhelices" of RecA-DNA filaments are similar to each other regardless the number of component filaments, and those formed on *Φ*x174 RFII dsDNA and pNEB206A dsDNA are measured as 339.3±6.2nm (690 counts of pitch/2) and 321.6±11.7nm (101 counts of pitch/2) respectively, consistent with earlier measurements made by electron microscopy with a much smaller sample size. The study of these structures provides insight into the self-interactions of RecA and RecA-like proteins, which are present in all

living cells, and into the general phenomenon of bundling, which is relevant to both biological and nonbiological filaments.

Introduction

In bacterial cells, RecA-like proteins are involved in homologous recombination and are recruited for SOS repair of massively damaged DNA.[1-5] In eukaryotic cells, homologous recombination is also closely connected to DNA repair and is assisted by proteins of the RecA/Rad51 family.[5-10] The ubiquity of RecA-like proteins in nature and the similarity among their functions indicate their common biological importance for DNA recombination, renaturation and repair. [1, 5]

The RecA protein forms active nucleoprotein filaments on single-stranded DNA (ssDNA) or double-stranded DNA (dsDNA) with nicks or single-stranded regions in the presence of ATP. It can also form inactive filaments in the absence of DNA and ATP or its analogues and/or presence of ADP.[11-15] Binding of ATP to RecA proteins introduces conformational changes that allow the RecA-ATP complex to bind primary DNA and form active filaments which play an important role during homologous pairing and strand exchange.[1, 2, 4, 5]

Structures of both active and inactive filaments are revealed by Small Angle Neutron Scattering (SANS), X-Ray Diffraction (XRD), Electron Microscopy (EM) and Atomic Force Microscopy (AFM).[11-17] The active nucleoprotein filament formed by RecA and ssDNA is responsible for the initiation of homologous pairing by invading a dsDNA molecule, after which strand-exchange occurs, followed by ATP hydrolysis which induces the dissociation of RecA.[1, 2, 4, 5] Three-strand or four-strand exchange

interactions between RecA-DNA nucleoprotein filaments and a second naked dsDNA have been detected by Fluorescence Resonance Energy Transfer (FRET), gel electrophoresis, EM and AFM.[14, 18-22]

In vitro studies show that the formation of active nucleoprotein filaments on nicked dsDNA is a two-step process.[2, 17] The first step is nucleation of RecA proteins at a single-stranded region, which is slow and rate-limiting, and the second is the much faster elongation of the filament from the nucleus. Both steps are facilitated by locally high concentrations of RecA proteins.[2]

Despite intensive study of the conformations of single RecA-DNA filaments and the strand-exchange intermediates, little attention has been paid to the interactions between RecA filaments except for studies of filamentous bundles[23, 24] and coaggregates[3, 25, 26]. Direct imaging of interactions between RecA-DNA filaments or aggregates of RecA-DNA filaments is even less frequent. A recent EM study revealed large parallel assemblies of RecA-dsDNA filaments in response to DNA damage *in vivo*, strengthening the likelihood of a biological role for the attraction between RecA-DNA filaments when DNA is damaged.[3] Self-"supercoiling" of circular RecA-dsDNA filaments has been observed *in vitro*[27], and "supercoiled" bundles of 3 or 6 RecA-dsDNA filaments were reported as the main products *in vitro* at moderate Mg^{2+} concentration and incubation time based on limited EM data[23, 24]. Detailed structures of "superhelical" bundles were given, but these structures were averaged over a very small number of individual bundles.[23, 24] In the same study, RecA-ssDNA filaments were observed to form bundles of many filaments without "supercoiling".[24] This conformational difference was attributed to the difference in the number of units per helical turn in these two types of RecA-DNA

filaments, specifically, the non-integral number of proteins per helical turn for dsDNA filaments and a near integral number for ssDNA filaments.[24] The slow hydrolysis of the cofactor, adenosine 5'-(γ-thio) triphosphate (ATPγS), was responsible for a correspondingly slow conformational change of RecA-DNA filaments in the bundles.[23] Although no apparent biological role for such aggregation was established in these studies, a thorough understanding of filament aggregation can provide valuable information regarding the biophysical and biochemical properties of RecA-DNA filaments *in vitro*, and eventually provide data to test molecular models of RecA self assembly**.** By using AFM, we are able to accumulate enough data for a statistical analysis of the bundle structure. Additionally, other features and conformations of bundles of RecA-dsDNA filaments are revealed, which have not been noticed before by EM.

Materials and Methods

Protein, DNA, and other reagents

Escherichia coli RecA protein, nicked circular *Φ*x174 RFII dsDNA (5386 base pairs) and linear pNEB206A dsDNA (2706 bases, with single stranded overhang) were purchased from New England Biolabs. RecA protein (2mg/ml) was used as received without further purification. ATPγS (Sigma) was prepared at a concentration of 2mg/ml by addition of reaction buffer (7mM $MgCl_2$, 100mM NaCl, 10 mM Tris-HCl 1mM EDTA, pH 8.0) or of 4mg/ml by addition of reaction buffer without $MgCl_2$ (100mM NaCl, TE, pH 8.0). In all preparations, molecular-biology-grade water (Eppendorf) was used and DNA was diluted with TE buffer (pH 8.0).

Filament formation, AFM imaging, and analysis

In brief, 12μg of ATPγS solution was mixed with 1.6μg of RecA and the appropriate amount of DNA in a total volume of 15ul (7mM $MgCl_2$, 100mM NaCl, Tris-EDTA, pH 8.0), which yields a ratio of about 2 DNA base pairs per RecA monomer. The reaction mixtures were incubated at 37^{o}C for one hour. For negative control, the reaction was conducted in the absence of DNA. A series of reactions were also carried out for one hour on RecA and *Φ*x174 RFII dsDNA system with Mg^{2+} concentrations ranging from 0mM to 48mM. With all other reaction conditions held fixed, the incubation time was varied from 1hr to 9 days to study its impact on the aggregation of filaments of RecA and *Φ*x174 RFII dsDNA at 7mM Mg^{2+}. After incubation, all reaction mixtures were immediately diluted with 85μl of AFM imaging buffer (10mM $MgCl_2$, 10mM NaCl, Tris-EDTA, pH 8.0). The resulting diluted mixtures were further diluted by 16 or 8 fold with imaging buffer for better imaging by AFM because higher concentrations of unreacted proteins prevents imaging other structures on the surface. The above diluted reaction mixtures were immediately deposited onto freshly pealed mica surfaces and incubated at room temperature for 4 minutes followed by thorough washing with molecular biology grade water and air drying before being mounted onto the AFM stage. A Multimode AFM with Nanoscope IIIa controller (Digital Instruments/Veeco) was used to image the sample in tapping mode in air with silicon probes NSC 16 (Mikromash). The resonance frequency of the cantilever was tuned to 150~170 kHz, and the drive amplitude and set point were adjusted to minimize the possible damage to the sample while maintaining stable image quality. The resulting images were first flattened with Nanoscope IIIa

software and further processed with Wsxm free software (developed by Nanotec Electrónica in Spain and downloadable at http://www.nanotec.es).

Images of intact DNA were obtained by a similar process. In general, DNA was first diluted with imaging buffer to 500pg/μl and then deposited in the same way as the RecA-DNA reaction mixtures.

Results and Discussion

Formation of complete filaments and control experiments

While the fixation of DNA onto mica surfaces by divalent ions is a complicated process[28], our experience shows that the imaging buffer we use holds the DNA and RecA-DNA filaments onto freshly pealed mica surfaces firmly and allows stable imaging in air. (See Supporting Information for reaction and sample preparation) Typical conformations of naked *Φ*x174 RFII dsDNA (5386bps, circular) on the mica surface are shown in Figure 3.1 (a). Most of the DNA molecules are circular, although linear DNA can occasionally be seen due to the breakage of plasmid circles.[29] Images of pNEB206A dsDNA (2706 bps, linear) were also obtained but not shown here. The mixture of RecA incubated with ATPγS without the addition of DNA shows that RecA proteins without DNA only form ring-like structures (Figure 3.1 (b)), which is consistent with earlier reports that RecA or RecA-like proteins can polymerize into both rings and short rods at appropriate conditions.[7, 10, 30] The reaction mixture of RecA and *Φ*x174 RFII dsDNA after a one-hour incubation shows both naked DNA molecules and mature nucleoprotein filaments in linear and circular forms (Figure 3.1 (c)), green arrows point to naked DNA molecules), indicating possible breakage of plasmid circles during RecA binding. The

appearance of naked DNA in an excess of RecA is due to slow nucleation rate of RecA on dsDNA at pH above neutral.[2, 17] As a result of typical compression effect when samples are imaged in dry conditions using AFM, the apparent height of nucleoprotein filaments is about 2.5~3 nm, which still makes these filaments so prominent that naked DNA are obscured and can barely be seen on the same AFM image. Not surprisingly, immature filaments that are partially covered by RecA were also observed (Figure 3.1 (d)), in circular and linear forms; green arrow indicates the naked DNA tail). Individual filaments formed with pNEB206A linear dsDNA are shown in Figure 3.1 (e).

The intra-filament "supercoiling" and its left-handedness

In addition to the intact filaments seen above, a variety of "superhelical" bundles of filaments are seen for a wide range of incubation times and Mg^{2+} concentrations. These bundles exhibit 2, 3, 4 or more component filaments. Not all the helical structures of filaments presented in our image gallery show clear handedness, but those with distinguishable handedness are all left-handed. The helical structures with legible handedness on RecA-dsDNA presented in this report are selected from our image gallery generated from all reaction conditions where only Mg^{2+} and reaction time were varied and all other reaction parameters were held fixed. In addition**,** all images are topographical unless stated otherwise. To help visualize the left-handedness, we provide an example for a 2-filament superhelix (Figure 3.2) before presenting other experimental images. In a typical AFM image, a brighter pixel means a larger vertical dimension or higher altitude (Figure 3.2 (a)). If we focus on the crossing point (locally brightest region) of two segments of the same filament or two different filaments, namely, R_1 and R_2

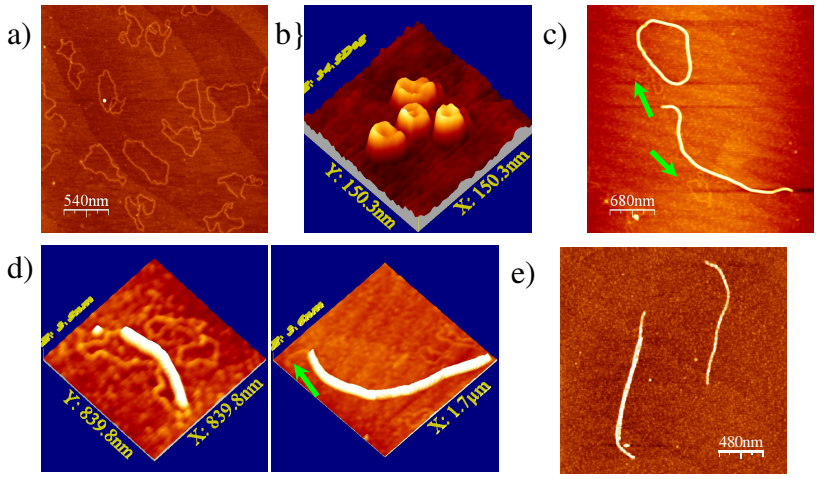

Figure 3.1. Formation of nucleoprotein filaments by DNA and RecA proteins. (a) Relaxed naked Φx174 RFII dsDNA (5386bps, circular) on surface. (b) Ring-like structures formed by RecA proteins without DNA (phase image). (c) RecA and Φx174 RFII DNA filaments in circular and linear forms with completely naked DNA in the background. The naked DNA molecules are barely visible and indicated with green arrows. (d) Partially formed RecA and Φx174 RFII DNA filaments in circular and linear forms. The naked tail (regions on DNA not covered by RecA) is indicated with green arrow. (e) RecA and pNEB206A dsDNA (2706 bps, linear) filaments. All reactions were conducted in Tris-EDTA buffer (pH 8.0) with 7mM $MgCl_2$ and 100mM NaCl for 1 hour.

(boxed area in Figure 3.2 (a); inset in Figure 3.2 (b)), the local arrangement of R_1 and R_2 is either R_1 on top of R_2 or R_2 on top of R_1. If R_1 is on top of R_2, which is left-handed rising, the local conformation of R_2 is flat on the bottom, but R_1 is bulged on the top. The opposite occurs if R_2 is on top of R_1 (right-handed rising). The line profile along filament R_1 exhibits a wider plateau than that along R_2 (Figure 3.2 (b)), implying that the bulge belongs to R_1. Hence, R_1 is on top of R_2 and the "supercoiling" is left-handed (see 3D rendering in Figure 3.2 (c)). The alignment of this bulge relative to the central axis S, therefore, clearly shows the handedness of the entire superhelix. The same method can be applied to cases involving more than two filaments. Intra-filament "superhelices" or self-coiled filaments, a specific form of 2-filament "superhelices", are only seen on RecA and Φx174 RFII DNA filaments both in linear and circular forms (Figure 3.2 (a); Figure 3.3). Self-interwinding was seen for circular RecA-dsDNA filaments in EM studies without mentioning the handedness[27]. Our AFM images show clear left-handedness for self-coiling (Figure 3.3 (a) and 3.3 (b)), but tighter self-coiling could yield illegible handedness (Figure 3.3 (c)). We note that both mature and immature linear RecA-dsDNA filaments can also self-interwind, which has not been reported before (Figure 3.3 (d), green arrow refers to the naked dsDNA tail of an immature filament).

The inter-filament "supercoiling"

Both filaments of Φx174 RFII DNA and pNEB206A DNA with RecA are able to interwind with other filaments to form inter-filament "superhelices" (Figure 3.4). Our results revealed the separate existence of bundles of 2 filaments (Figure 3.4 (a), pNEB206A filaments; Figure 3.4 (b) and green rectangular area in Figure 3.4 (c), Φx174

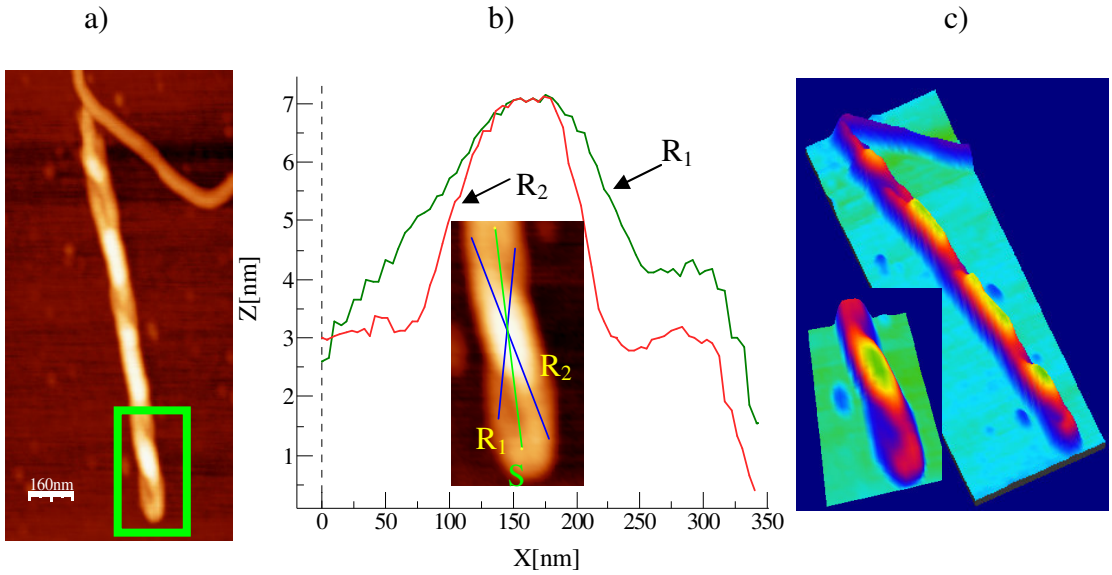

Figure 3.2. Observation of left-handedness in plane images. (a) Plane image of coiled filaments of RecA and Φx174 RFII DNA at a reaction time of around 2 days at 7mM Mg^{2+}; (b) Topographic profiles of segment R_1 and R_2 at an R_1-R_2 crossing. The wider plateau in the profile of R_1 indicates that R_1 is on top of R_2 and bulges out, making a left-handed helical turn. Inset: enlarged image of boxed area in (a), S stands for the central axis of "supercoiling"; (c) Left-handedness is clearly seen in a 3D reconstruction.

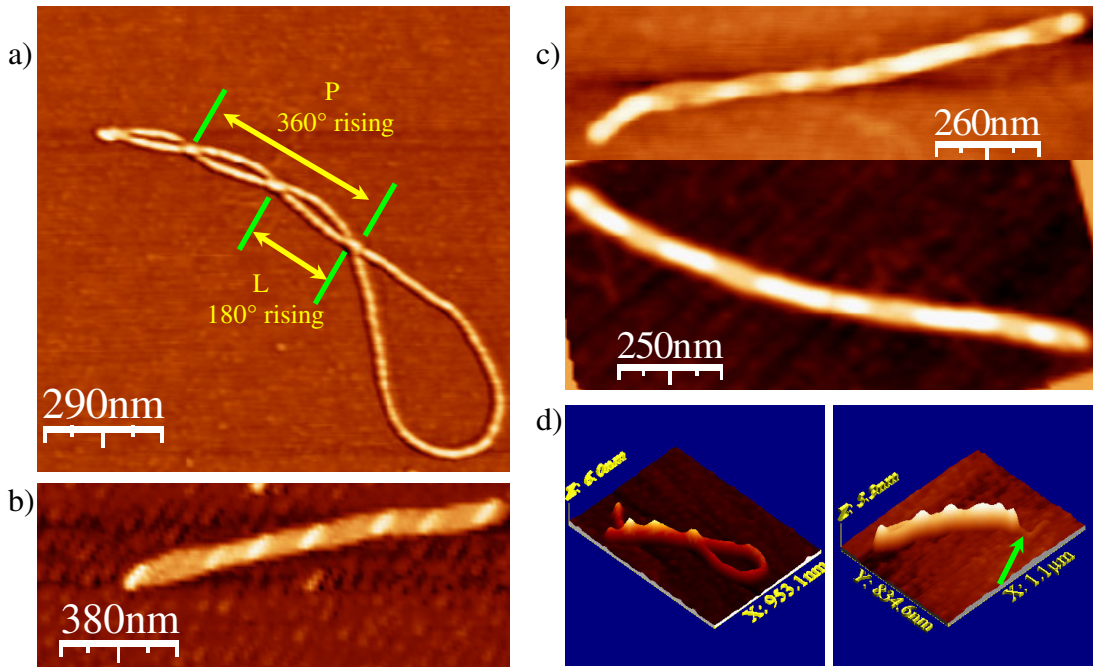

Figure 3.3. Formation of intra-filament "superhelices" by RecA and Φx174 RFII DNA filaments. (a) Self-coiling of circular filaments with legible left-handedness. L is the path between two adjacent crossing points (180° helical rising), P is the "superhelical" pitch (360° helical rising); 2mM Mg^{2+} and 1 hour reaction time; phase image. (b) Self-coiling of circular filaments with legible left-handedness, 7mM $Mg^{2+}$and 1hour reaction. (d) Compact self-coiling of circular filaments with unclear handedness. Upper image: 1-hour reaction at 7mM Mg^{2+}; lower image: 1-hour reaction at 48mM Mg^{2+}. (d) Self-coiling of mature (left) and immature (right) linear filaments, both after 1hour reaction with 7mM Mg^{2+}. Green arrows indicate the naked DNA tails.

RFII DNA filaments), which is not reported by EM studies other than 2-filament self-coiling, i.e., a single filament wrapping once around itself. For instance, it is clear that a linear filament (both its ends are indicated with green arrows) winds around a circular filament in Figure 3.4 (b). These 2-filament bundles occur frequently and could further wind into 4- or 6-filament bundles (Figure 3. 4 (c), green rectangle and circle), consistent with conformational changes induced by hydrolysis of ATPγS where 2-filmaent and 3-filament bundles have been found to be components of 6-filament bundles.[23] Interestingly, the further "supercoiling" of intra-filament "superhelices" creates unique 4-filament bundles, or "super-superhelices", which exhibit 3 levels of helical structures, the right handed building blocks of RecA-dsDNA filaments, left-handed self-coiling of individual filaments and left-handed inter-winding of 2 self-coiled filaments (Figure 3.4 (d), each individual self-coil filament is numbered). There are two such "super-superhelices" in Figure 3.4 (d), namely, self-coiled filaments 1&2 (or 3&4) interwind with each other to form "super-superhelices". Finally, large bundles of filaments were more frequently seen at higher Mg^{2+} concentrations, where regions composed of different numbers of filaments are shown in a single large bundle (Figure 3. 4 (e)).

Pitches of the "supercoils"

To characterize these "superhelical" bundles, it is essential to determine the "superhelical" pitch statistically. Paths (L) between two neighboring crossing points on "superhelical" bundles were collected on bundles formed at 7mM Mg^{2+} with reaction time ranging from 1 hour to 9 days so that the pitch can be obtained in the way described in the following paragraph. By definition, the pitch P is the distance along the helical axis

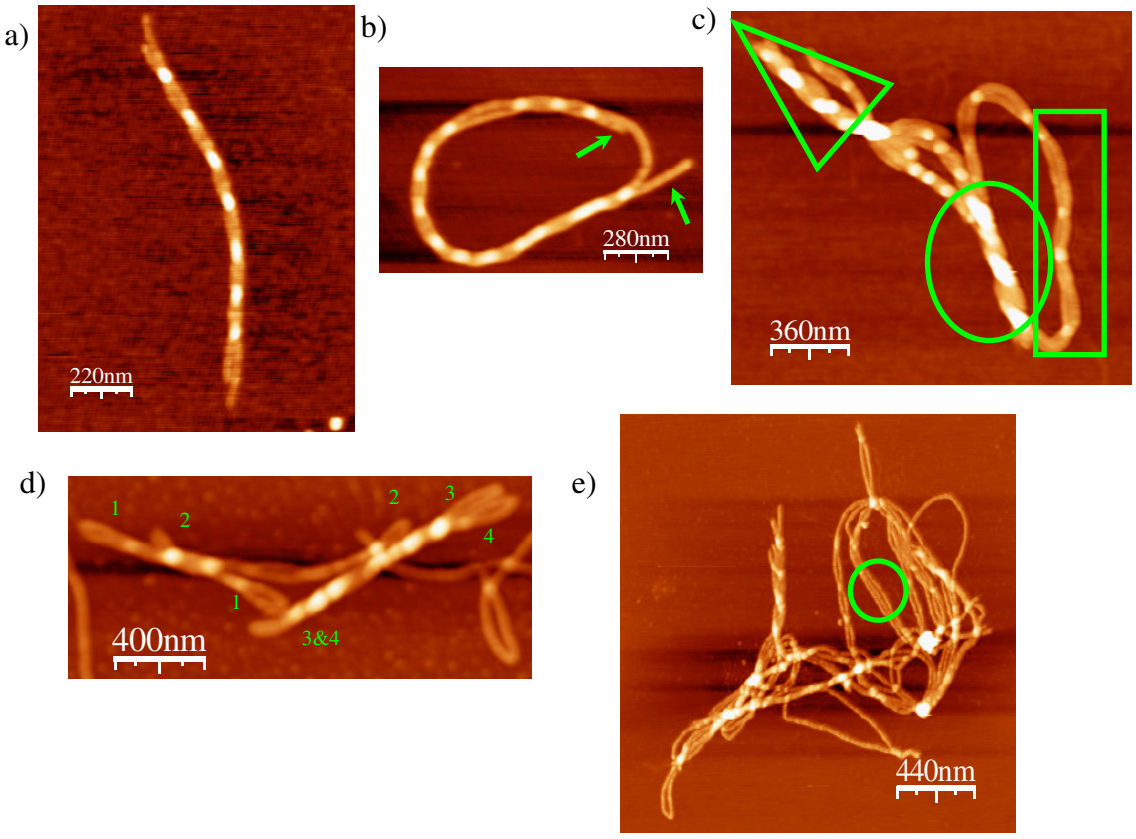

Figure 3.4. Inter-filament "superhelices" formed by coiling of RecA-dsDNA filaments. (a) 2-filament helical bundle of RecA and pNEB206A DNA, 1-hour reaction at 7mM Mg^{2+}; (b) 2-filament helical bundle of RecA and Φx174 RFII DNA. Green arrows refer to the ends of the linear component filament, 1 hr reaction at 7mM Mg^{2+}; (c) Bundles of RecA and Φx174 RFII DNA show 2-filament bundles (green Box), which further coil into 4-filament and 6-filament (green triangle and circle) left-handed "supercoils". Reaction is conducted at 36mm Mg^{2+} for 1 hour; (d) "Super-superhelices" formed by coiling of RecA and Φx174 RFII DNA intra-filament "superhelices" during 1 hour reaction at 7mM Mg^{2+}; numbers refer to different filaments and identity their ends. It is clear that self-coiled filaments 1&2 (or 3&4) interwind with each other to form "super-superhelices"; (e) Large left-handed helical bundle of RecA and Φx174 RFII DNA filaments formed after 1 hour reaction with 24mM Mg^{2+}. Regions with different numbers of component filaments can be seen; filaments in green circles are parallel to each other locally.

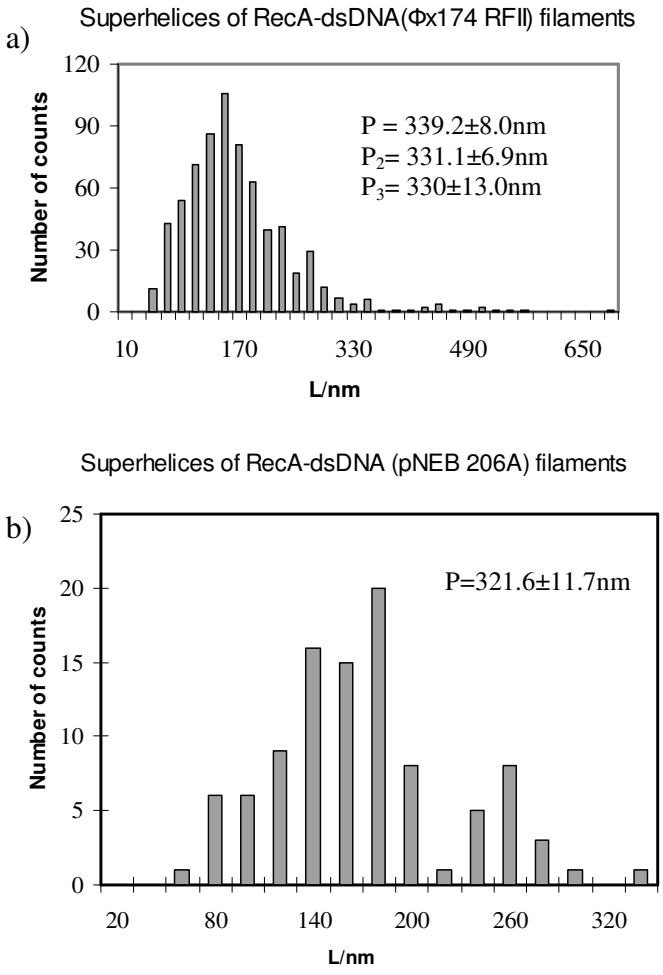

Figure 3.5. "Superhelical" pitches of bundles of RecA-dsDNA filaments. (a) Distribution of L from "superhelical" bundles of RecA and Φx174 RFII DNA filaments. Pitches are collected from 3 groups of bundles, that is, P_2 from 2-filament bundles, P_3 from 3-filament bundles and P_O from all other bundles. P is the value averaged over all data; (b) Distribution of L from "superhelical" bundles of RecA and pNEB206A DNA filaments. Due to smaller sample size, data are not divided into groups; only the value of pitch averaged over all data is given.

over which the filament makes a 360° turn. Therefore, L is equal to P/2, since crossing points occur with every 180° turn (Figure 3.3 (a)). The distributions of L sampled from all bundles of RecA filaments on Φx174 RFII DNA (N=690) and pNEB206A dsDNA (N=101) are shown in Figure 3.5 (a) and 3.5 (b) respectively, where N is the number of counts. The wide distributions in both cases (standard deviations equal to 79.1nm and 58.6nm for the two RecA-dsDNA systems respectively) are possibly the consequence of the gradual formation of "superhelical" bundles via random contact. One might suspect that the variation in pitches arises from a later slow internal conformational adjustment induced by slow hydrolysis of ATPγS which occurs over a time scale of hours. However, it has been shown that this adjustment of conformation generates little variation in the "superhelical" pitch, according to EM studies.[23, 24] In the same studies, there is also little variation detected among the "superhelical" pitches for 3-filament, 6-filament and 5-filament bundles.[23, 24] Our results support the conclusion that the pitches of bundles with different numbers of component filaments are similar. If the 690 samples counted on RecA-(Φx174 RFII DNA) filaments are separated into 3 groups, that is, 2-filament bundles, 3-filament bundles and all other bundles, the average pitches of 2-filament bundles (P_2) and 3-filament bundles (P_3) are 331.1±6.9nm (N=391) and 330±13.0nm (N=111) respectively, while that of all other bundles (P_O) is 361.3±15.1nm (N=188). At this point, the value of P averaged over all "superhelical" bundles of RecA and Φx174 RFII DNA filaments, 339.2±8.0nm, is reasonably taken as the characteristic value of P for these bundles. It is not surprising that the pitch of bundles of RecA with pNEB206A dsDNA filaments is 321.6±11.7nm, close to that of Φx174 RFII DNA filaments. The value of P claimed by earlier studies from limited data is about 340nm, while 378nm is

calculated from their data for 3-filament bundles (N=several), and a range of 326nm~487nm can be inferred for 6-filament bundles (N=13), or 324nm for 5-filament bundles (N=1).[23, 24]

Conclusions

We have found that RecA-dsDNA filaments aggregate into "supercoiled" bundles with regular pitches using AFM. The packaging of RecA-DNA filaments is apparently directed by the attraction of RecA molecules to each other in the presence of magnesium ions, as supported by other studies involving protein-induced DNA bending.[16] The formation of left-handed bundles of RecA-dsDNA has been attributed to the non-integral number of units per helical turn in RecA-dsDNA filaments, which supports formation of multi-filament bundles over a range of Mg^{2+} concentration. RecA-ssDNA filaments only form non-"supercoiling" aggregates because of their nearly integral number of protein units per helical turn.[24] Our results show other conformations of RecA-dsDNA filaments, namely, 2-filament bundles and their further-coiling products, but that does not exclude the occasional occurrence of locally parallel alignment of filaments (circled area in Figure 3.4 (e)) which is also consistent with *in vivo* studies where RecA-dsDNA filament were seen in parallel conformation in response to severe DNA damage.[3] Statistical analysis of our data shows that these bundles exhibit similar "superhelical" pitches despite the different numbers of component filaments. Although homology in DNA sequence is required for strand exchange, which is the biological function of RecA, homology is apparently not necessary for the aggregation of RecA-DNA filaments into "superhelical" bundles. This conclusion follows from our observation of self aggregation

of RecA-DNA filaments within a single circular DNA sequence, which lacks sequence homology over extended distances. In addition, our studies provide insight into the general mechanism of supercoiling and supercoiled aggregation, which also occurs in DNA[31, 32] and nonbiological charged polymers.[33]

References

1. Kowalczykowski, S. C.; Eggleston, A. K., "Homologous pairing and DNA strand-exchange proteins", Annual Review of Biochemistry, 63991-1043 (1994)

2. Cox, M. M., "Binding two DNA molecules at once: the RecA protein" in: Revzin A. (eds.), "The biology of nonspecific DNA-protein interactions" CRC Press, Boca Raton, U.S.A, 1990, 171-196

3. Levin-Zaidman, S.; Frenkiel-Krispin, D.; Shimoni E.; Sabanay, I.; Wolf, S. G.; Minsky, A., "Ordered intracellular RecA-DNA assemblies: A potential site of in vivo RecA-mediated activities", Proceeding of the National Academy of Sciences of The United States of America 97, 6791-6796 (2000)

4. Egelman, E. H., "A tale of two polymers: new insights into helical filaments", Nature Reviews Molecular Cell Biology 4, 621-630 (2003)

5. West, S. C., "Molecular views of recombination proteins and their control", Nature Reviews Molecular Cell Biology 4, 435-445 (2003)

6. Mazina, O. M.; Mazin, A.V., "Human Rad54 protein stimulates DNA strand exchange activity of hRad51 protein in the presence of Ca2+", Journal of Biological Chemistry 279, 52042-52051 (2004)

7. Kinebuchi, T.; Kagawa, W.; Enomoto, R.; Tanaka, K.; Miyagawa, K.; Shibata, T.; Kurumizaka, H.; Yokoyama, S., "Structural basis for octameric ring formation and DNA interaction of the human homologous-pairing protein Dmc1", Molecular Cell 14, 363-374 (2004)

8. Yu, X.; Jacobs, S. A.; West, S. C.; Ogawa, T.; Egelman, E. H., "Domain structure and dynamics in the helical filaments formed by RecA and Rad51 on DNA", Proceeding of the National Academy of Sciences of The United States of America 98, 8419-8424 (2001)

9. Shin, D. S.; Chahwan, C.; Huffman, J. L.; Tainer, J. A., "Structure and function of the double-strand break repair machinery", DNA Repair 3, 863-873 (2004)

10. Passy, S. I.; Yu, X.; Li, Z.; Radding, C. M.; Masson, J. Y.; West, S. C.; Egelman, E. H., "Human Dmc1 protein binds DNA as an octameric ring" Proceeding of the National Academy of Sciences of The United States of America 96, 10684-10688 (1999)

11. Xing, X.; Bell, C. E., "Crystal structures of Escherichia coli RecA in a compressed helical filament", Journal of Molecular Biology 342, 1471-1485 (2004)

12. VanLoock, M. S.; Yu, X.; Yang, S.; Lai, A. L.; Low, C.; Campbell, M. J.; Egelman, E.H., "ATP-Mediated conformational changes in the RecA filament", Structure 11, 187-196 (2003)

13. Story, R. M.; Weber, I. T.; Steitz, T. A., "The structure of the escherichia-coli RecA protein monomer and polymer", Nature 355, 318-325 (1992)

14. Egelman, E. H.; Stasiak, A., "Electron-microcopy of RecA-DNA complexes -2 different states, their functional-significance and relation to the solved crystal-structure", Micron 24, 309-324 (1993)

15. Dicapua, E.; Schnarr, M.; Ruigrok, R. W.; Lindner, P.; Timmins, P. A., " Complexes of RecA protein in solution – a stuy by small-neutron-scattering", Journal of Molecular Biology 214, 557-570 (1990)

16. Lyubchenko, Y. L.; Jacobs, B. L.; Lindsay, S. M.; Stasiak, A., "Atomic force microscopy of nucleoprotein complexes", Scanning Microscopy 9, 705-727 (1995)

17. Sattin, B. D.; Goh, M. C., "Direct observation of the assembly of RecA/DNA complexes by atomic force microscopy", Biophysical Journal 87, 3430-3436 (2004)

18. Xiao, J.; Singleton, S. F., "Elucidating a key intermediate in homologous DNA strand exchange: Structural characterization of the RecA-triple-stranded DNA complex using fluorescence resonance energy transfer", Journal of Molecular Biology 320, 529-558 (2002)

19. Seong, G. H.; Niimi, T.; Yanagida, Y.; Kobatake, E.; Aizawa, M., "Single-molecular AFM probing of specific DNA sequencing using RecA-promoted homologous pairing and strand exchange", Analytical Chemistry 72, 1288-1293 (2000)

20. Jain, S. K.; Cox, M. M.; Inman, R. B., "Occurrence of 3-stranded DNA within a RecA protein filament", Journal of Biological Chemistry 270, 4943-4949 (1995)

21. Gamper, H. B.; Hou, Y. M.; Kmiec, E. B., "Evidence for a four-strand exchange catalyzed by the RecA protein", Biochemistry 39, 15272-15281 (2000)

22. Reddy, M. S.; Vaze, M. B.; Madhusudan, K.; Muniyappa, K., "Binding of SSB and RecA protein to DNA-containing stem loop structures: SSB ensures the polarity of RecA polymerization on single-stranded DNA", Biochemistry 9, 14250-14262 (2000)

23. Yu, X.; Egelman, E. H., "Direct visualization of dynamics and co-operative conformational changes within RecA filaments that appear to be associated with the hydrolysis of adenosine 5′-O-(3-thiotriphosphate)", Journal of Molecular Biology 225, 193-216 (1992)

24. Egelman, E. H.; Stasiak, A., "Structure of helical RecA-DNA complexes - II. Local conformational changes visualized in bundles of RecA-ATPγS filaments", Journal of Molecular Biology 200, 329-349 (1988)

25. Gonda, D. K; Radding, C. M., “The mechanism of the search for homology promoted by recA protein - facilitated diffusion within nucleoprotein networks”, Journal of Biological Chemistry 261, 13087-13096 (1986).

26. Pinsince, J. M.; Griffith, J. D., “Early stages in RecA protein-catalyzed pairing - Analysis of coaggregate formation and non-homologous DNA contacts”, Journal of Molecular Biology 228, 409-420 (1992)

27. Webb, B. L.; Cox, M. M.; Inman, R. B., “An interaction between the Escherichia coli RecF and RecR proteins dependent on ATP and double-stranded DNN”, Journal of Biological Chemistry 270, 31397-31404 (1995)

28. Pastré, D.; Piétrement, O.; Fusil, S.; Landousy, F.; Jeussset, J.; David, M.; Hamon, L.; Cam, E.; Zozime, A., “Adsorption of DNA to mica mediated by divalent counterions: a theoretical and experimental study”, Biophysical Journal 85, 2507-2518 (2003)

29. Marguet, E.; Forterre, P., “DNA stability at temperatures typical for hyperthermophiles”, Nucleic Acids Research 22, 1681-1686 (1994)

30. Lee, M. H.; Leng, C. H.; Chang, Y. C.; Chou, C. C.; Chen, Y. K.; Hsu, F. F.; Chang, C. S.; Wang, A. H.; Wang, T. F., “Self-polymerization of archaeal RadA protein into long and fine helical filaments”, Biochemical and Biophysical Research Communications 323, 845-851 (2004)

31. Vologodskii, A. V.; Levene, S. D.; Klenin, K. V.; Frank-Kamenetskii, M. D.; Cozzarelli., N. R., “Conformational and thermodynamic properties of supercoiled DNA”, Journal of Molecular Biology 228, 1224-1243 (1992)

32. Rybenkov, V. V.; Vologodskii, A. V.; Cozzarelli, N. R., “The effect of ionic conditions on the conformations of supercoiled DNA .1. Sedimentation analysis”, Journal of Molecular Biology 267, 299-311 (1997)

33. Cornelissen, J .J .L. M.; Fischer, M.; Sommerdijk, N. A. J. M.; Nolte, R. J. M. , “Helical superstructures from charged poly(styrene)-poly(isocyanodipeptide) block copolymers”, Science 280, 1427-1430 (1998)

CHAPTER IV
RECA-SSDNA FILAMENTS "SUPERCOIL" IN THE PRESENCE OF SINGLE-STRANDED DNA BINDING PROTEIN

Chapter Summary

We find that RecA-ssDNA filaments, in the presence of single-stranded DNA binding (SSB) protein, organize into left-handed bundles, which differ from the previously reported disordered aggregates formed when SSB is excluded from the reaction. In addition, we see both left- and right-handedness on bundles of two filaments. These two-filament "supercoils", individual filaments, and other smaller bundles further organize into more complicated bundles, showing overall left-handedness which cannot be explained by earlier arguments that presumed "supercoiling" is absent in RecA-ssDNA filaments. This novel finding and our previous results regarding "supercoling" of RecA-dsDNA filaments are, however, consistent with each other and can possibly be explained by the intrinsic tendency of RecA-DNA filaments, in their fully-coated form, to order themselves into helical bundles, independent of the DNA inside the filaments (ssDNA or dsDNA). RecA-RecA interactions may dominate the bundling process, while the original conformation of DNA inside filaments and other factors (mechanical properties of filaments, concentration of filaments, and Mg^{2+} concentration) could contribute to the variation in the appearance and pitch of

"supercoils". The tendency of RecA-DNA filaments to form ordered "supercoils" and their presence during strand exchange suggest a possible biological importance of "supercoiled" filaments.

Introduction

Homologous recombination and repair of damaged DNA are essential biological functions in living organisms. These processes require participation of many proteins, including RecA (Recombinase A) or RecA-like proteins.[1-3] It is well known that RecA proteins form helical nucleoprotein filaments on single-stranded DNA (ssDNA) or double-stranded DNA (dsDNA) in the presence of ATP or its analogs and that the filaments function as active substrates to initiate homologous recombination or strand exchange interactions with other naked dsDNA molecules, which serves as part of the DNA damage repair mechanism[2, 4]. The formation of filaments on DNA molecules involves two steps, nucleation and extension. The nucleation on dsDNA is slower than that on ssDNA and the presence of a single-stranded region on dsDNA can enhance the nucleation process, while the extension of filaments is fast on both dsDNA and ssDNA.[2] Secondary structures on ssDNA tend to block filament extension, resulting in incomplete RecA coating, especially for long ssDNA molecules.[5] Hence, single stranded DNA binding (SSB) protein is usually added to remove secondary structures within ssDNA.[5, 6] Although SSB protein competes with RecA for nucleation sites on ssDNA, it is readily removed by RecA when the extension of RecA from other nucleation sites reaches SSB binding sites.[5-7] In addition, free SSB protein possibly assists strand exchange by binding the outgoing single-stranded DNA and thus prevents the reversal of strand

exchange.[8]

It is believed that the search for homologous regions is facilitated by coaggregation of RecA-filaments with target naked DNA molecules, during which a highly efficient, but enigmatic, screening for homology occurs.[2] Earlier studies on coaggregates or bundles of RecA-filaments show no direct evidence of any biological role of filament-filament aggregation, which has limited interest in this topic for the last decade.[9-11] Recently, however, an *in vivo* study has indicated that such aggregation could be related to the cellular response to massive DNA damage.[12] RecA-DNA filaments and aggregates visualized with electron microscopy (EM) [11-13] and AFM [14-16] have shown that RecA-dsDNA filaments readily assembly into left-handed bundles [11, 14]. RecA-ssDNA filaments aggregate as well, but have in the past always been found to be in a disordered conformation.[11] However, we show here that RecA-ssDNA filaments can form left-handed "supercoils" if complete coating of ssDNA by RecA is ensured by inclusion of SSB protein. And these "supercoils" also exist during the limited strand-exchange interaction that occurs in the presence of adenosine 5′-O-(3-thiotriphosphate) (ATPγS), a nearly non-hydrolysable version of ATP. Surprisingly, the coexistence of left- and right-handedness on a single bundle is seen on two-filament bundles of RecA-ssDNA filaments, which is absent in bundles of RecA-dsDNA filaments.

Materials and Methods

The experimental procedure is similar to that of our previous study [14] except that homologous dsDNA fragments with different lengths were added to initiate limited strand exchange with a 5386-bp viron ssDNA.

Protein, DNA, and other reagents

Escherichia coli RecA protein, nicked circular *Φ*x174 RFII dsDNA (5386 base pairs), supercoiled *Φ*x174 RFI dsDNA, circular *Φ*x174 viron ssDNA (5386 bases), pNEB 206A dsDNA, DNA ladders, Proteinase K and six restriction enzymes (*BssH* II , *Drd* I, *Sap* I, *Bts* I, *Ssp* I, *BsoB* I) were purchased from New England Biolabs. Single stranded DNA binding protein (1–5mg/ml) was purchase from Promega. RecA protein (2mg/ml) was used as received without further purification. ATPγS and SDS were purchased from Sigma. In all preparations, molecular-biology-grade water (Eppendorf) was used and DNA was diluted with TE buffer (pH 8.0).

Preparation of linear dsDNA fragments and strand exchange interactions

A series of restriction fragments were prepared by double digestion of *Φ*x174 RFI dsDNA with *BssH* II and one of the remaining 5 restriction enzymes, and the resulting fragments were separated by agarose gel electrophoresis and collected using a Qiagen Gel extraction kit. The concentrations of these fragments were estimated by reading their brightness on the gel and using DNA ladders as reference. *Φ*x174 viron ssDNA was first incubated with RecA protein for 10 minutes at 37 ^{o}C, and SSB protein and ATPγS were then added to initiate filament formation. After another 20 minutes, dsDNA fragments were introduced to initiate strand exchange interaction. That moment is also set as the starting point of sampling. The final reaction volume is 20 μL, containing 1.4 nM viron DNA, 2.65 μM RecA, 3 mM ATPγS, 400 nM SSB in 1x RecA buffer (10 mM $MgCl_2$, 70 mM Tris-HCl, 5 mM Dithiothreitol, pH 7.6). A 6 μL sample was taken out at 0 min, 40 min and 180 min respectively, 1 μL of which was diluted 10 times with 1x RecA buffer,

deposited onto mica surface immediately for 5 min and dried by air blowing. AFM imaging and analysis are identical to our previous study. The remaining sample was deproteinized in 1% SDS and 1 mg/ml Proteinase K for 30 min at 37 ^{o}C and then frozen before running on agarose gel.

Results and Discussion

According to the gel images (not shown), limited strand exchange did occur under our reaction conditions, which has been already shown by other groups.[17, 18] In the presence of SSB protein, regular filaments together with "supercoiled" bundles are seen in all cases by AFM. Some typical regular filaments are shown in Figure 4.1 (a) where the contour length is approximately 150 percent of that for B-form dsDNA. The observed linear filaments are caused by either impurities of as-received circular ssDNA or breakage during sample preparation.

RecA-ssDNA filaments form "supercoiled" bundles in the presence of SSB

Strikingly, almost all bundles with discernable handedness are composed of multiple filaments and are biased towards left-handedness except for a few observable cases of right-handedness on two-filament bundles which will be discussed in a later section. Some typical bundles pictured at various conditions are shown in Figure 4.1 (b) and 4.1 (c). The appearance of left-handed bundles is not in conflict with a previous EM report that RecA-ssDNA filaments only form disordered aggregates [11], since in the present study ssDNA was preincubated with SSB protein to facilitate RecA binding by removal of secondary structure in ssDNA, which was not added in the early study.

Hence, the filaments or aggregates of RecA and ssDNA reported previously would likely have been partially and discontinuously covered by RecA molecules, and thus not comparable to the current case, where filaments were likely fully coated by RecA. Other studies have demonstrated that, in the absence of SSB, ssDNA molecules form much shorter filaments in most circumstances due to barriers created by secondary structures of ssDNA [5, 16], which was also seen in our control experiment without SSB protein (Figure 4.1 (d) and 4.1 (e)). The contour length of filaments formed without SSB could be as short as 400 nm [16], less than 15% of that of fully-coated filaments. Apparently, these partially-coated filaments aggregate much differently than the fully-coated ones. This supports our inference that RecA-ssDNA filaments are capable of forming regular "supercoils" if the ssDNA is fully coated with RecA protein. Therefore, the SSB protein is indispensable to achieving "supercoiling" of RecA-coated ssDNA filaments. A partially-coated RecA-ssDNA filament is malformed and may yield disordered aggregates, as seen in the EM study. In contrast, SSB protein is not needed to form fully-coated filaments on dsDNA molecules. Consequently, one sees different behavior with RecA-dsDNA vs. RecA-ssDNA filaments during aggregation if no SSB protein is present. When RecA-ssDNA filaments are fully coated, such differences are reduced and left-handed "superhelical" bundles are visible just as for RecA-dsDNA filaments. There is no observable impact of SSB protein on the formation of "supercoils" in the RecA-dsDNA system (data not shown), which is reasonable since SSB protein only binds to ssDNA molecules.

Control experiments, in which water, homologous ssDNA, or heterologous dsDNA (pNEB 206A) was added instead of homologous dsDNA fragments, also yield

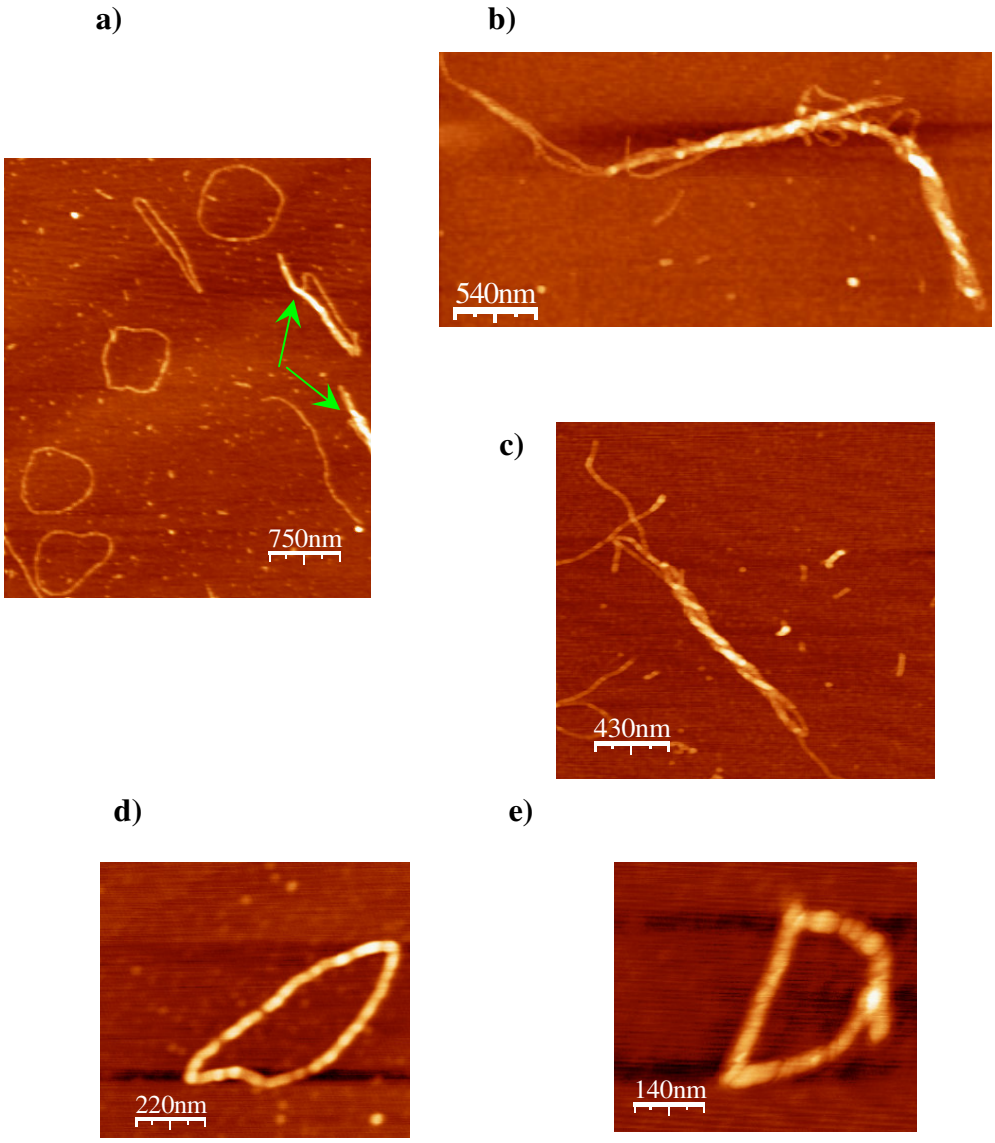

Figure 4.1. "Supercoiled" conformation of RecA-ssDNA filaments. (a) Fully coated RecA-ssDNA filaments in the presence of SSB. The image shown was taken 180 minutes after initiating strand exchange by addition of 200-bp fragments of dsDNA. Some coiled filaments are also seen in the image (green arrows); (b) & (c) Left-handed "supercoils" of RecA-ssDNA filaments during strand-exchange interaction with homologous dsDNA fragments of 1047 bps sampled at 180 min and 3790 bps at 0 min respectively; (d) & (e) Incomplete RecA-ssDNA filaments formed without SSB protein. The contour length of the filament in (d) is measured as 1.6 µm, while for the one in (e) it is only 950 nm. The contour length would be about 2.7 µm if the ssDNA is fully coated.

left-handed bundles with occasional right-handedness observable in two-filament "supercoils" (Figure 4.2). This result confirms that the "supercoiling" of RecA-ssDNA filaments is not due to the transfer of RecA molecules from ssDNA to dsDNA, but to an intrinsic "supercoiling" tendency possessed by both RecA-ssDNA filaments and RecA-dsDNA filaments. In other words, *it is an intrinsic property of RecA-DNA filaments to form "supercoils" whether the DNA inside is single or double stranded, provided that the DNA molecules are fully coated with RecA protein.* We suggest that the intra- and inter-filament contacts between RecA molecules are possibly the dominant factor that leads to the "supercoiling" of those bundles, tuned by divalent cations. Determining the detailed mechanism of bundle formation would require further experimental data. Incubation time, concentration of Mg^{2+}, filament concentration, and other factors, such as whether the enclosed DNA is single- or double-stranded, may contribute to the variability of the helical pitch of the "supercoiling" and the size of bundles.

The aggregation kinetics depends on the incubation time and Mg^{2+}

Our study of aggregation of RecA-dsDNA filaments shows that the both incubation time and Mg^{2+} concentration only impact the size of aggregates of RecA-dsDNA filaments but not the tendency to "supercoil". Upon increase of magnesium concentration, larger and more compact aggregates are more frequently seen, accompanied by a sharp decrease in the number of intact single filaments and simple complexes or small bundles. We counted the numbers of objects on a mica surface with a scan area of 40 μm × 40 μm at ten different locations for each reaction occurring at Mg^{2+} concentrations ranging from 0 to 48 mM with a one-hour incubation (Figure 4.3 (a)).

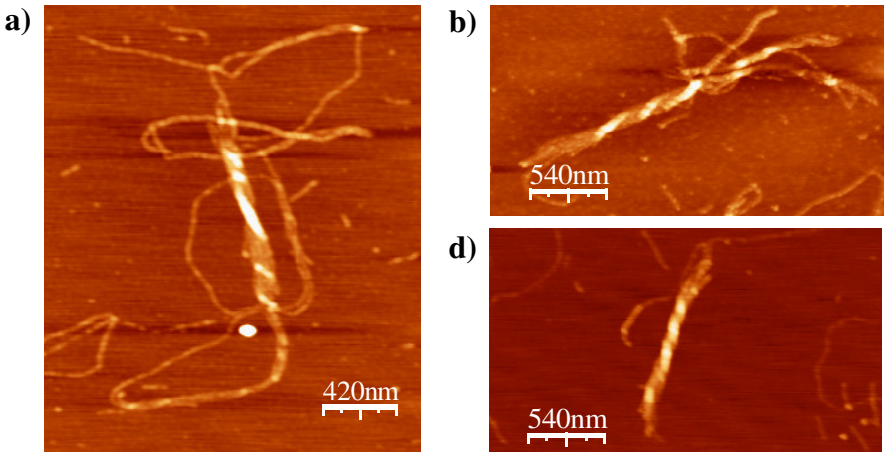

Figure 4.2. Left-handed "supercoils" formed in the absence of homologous dsDNA. Substitution of homologous dsDNA with (a) water, (b) homologous ssDNA, and (c) heterologous dsDNA still results in "supercoils" that are similar to those seen during strand exchange. The corresponding sampling times are (a) 40 min, (b) 180 min, and (c) 40 min.

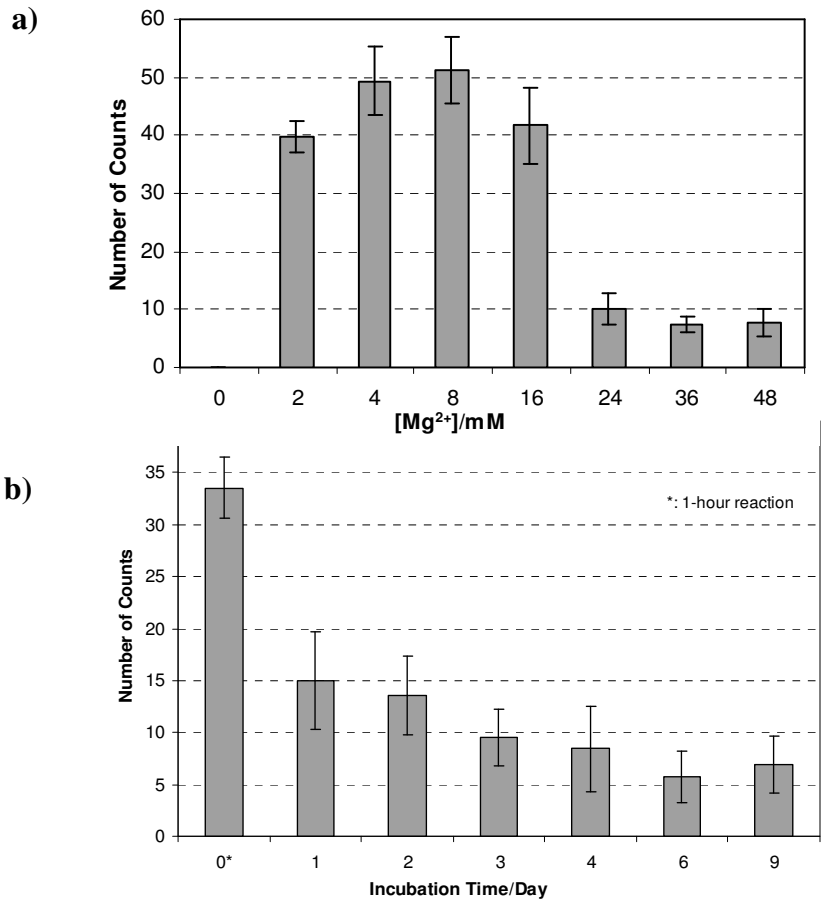

Figure 4.3. Effect of Mg^{2+} concentration and incubation time on the aggregation of RecA-dsDNA filaments. (a) Number of objects counted on a mica surface with a scan area of 40 μm × 40 μm averaged at ten different locations with incubation time of 1 hour at various Mg^{2+} concentrations. The initial increase at low Mg^{2+} levels is due to the enhanced formation of filaments, while the later decrease at high Mg^{2+} levels is the result of formation of large aggregates; (b) Number of objects counted on a mica surface with a scan area of 40 μm × 40 μm averaged at ten different locations decreases as incubation times increases from 1 hour to 9 days at 7 mM Mg^{2+}. The decrease indicates the gradual formation of large aggregates.

Although the resolution at such a large scanning area is too low to determine the detailed structure of an individual object, it still allows us to estimate the number of objects with visible length larger than 400 nm in the X-Y plane. No objects are observed when magnesium is absent, obviously due to lack of filament formation since magnesium is essential to activate RecA to coat DNA molecules. Once magnesium is present in the reaction, single filaments or bundles of filaments are seen and the number of counts reaches a maximum at a magnesium concentration of around 8 mM. A further increase in Mg^{2+} leads to a decrease in the number of objects, apparently due to more or faster aggregation in the presence of a higher concentration of Mg^{2+}. A yet further increase in magnesium concentration above 24 mM shows little impact on the number of objects counted, indicating that the effect of magnesium saturates at concentrations above 24mM. Similarly, denser packaging of RecA-dsDNA filaments can be seen when the incubation time is increased with Mg^{2+} concentration maintained at 7 mM. The number of objects counted gradually decreases, from around 34 counts in a one-hour reaction to less than 8 counts in reactions lasting more than 4 days (Figure 4.3 (b)), indicating the slow but accumulating merger of aggregates into larger ones. A similar trend is seen for RecA-ssDNA filaments when the incubation time is changed from 0 min to 180 min, which provides additional evidence that the aggregation of RecA-ssDNA filaments follows a mechanism similar to that for the aggregation of RecA-dsDNA filaments.

The aggregates are different for RecA-ssDNA and RecA-dsDNA filaments

Despite the overall similarity in the appearance of bundles of RecA-ssDNA (fully coated) and RecA-dsDNA filaments, bundles of RecA-ssDNA filaments exhibit some

unique features that are not seen for RecA-dsDNA filaments. Contact between filaments is tighter and denser on RecA-ssDNA than on RecA-dsDNA filaments. The component filaments within these "supercoils" of RecA-ssDNA tend to be tightly wrapped by their neighbors so that it is difficult to tell the exact number of filaments in a single bundle or the handedness (Figure 4.4 (a) and 4.4 (b)). In many cases, two filaments seem to "melt" into each other and might be mistaken as a single filament if there were no non-coiled filaments in the same scan (Figure 4.4 (a)) or apparently split of the "melted" coils (Figure 4.4 (b)). However, for dsDNA filaments, although we occasionally find "supercoiling" that is so tight that the two filaments are almost indistinguishable, we are still able to tell that there are two filaments instead of a single one without referring to non-coiled filaments, and handedness is readable in most cases. The greater flexibility of RecA-ssDNA filaments relative to RecA-dsDNA filaments is possibly a reason for the "melted" conformations of RecA-ssDNA filaments. As one can imagine, it would be easier for softer RecA-ssDNA filaments to coil tightly with each other than for stiffer RecA-dsDNA filaments to do so. Additionally, both handednesses were occasionally seen in a single bundle of two filaments (Figure 4.4 (c) and 4.4 (e)). This is never observed for RecA-dsDNA filaments. A couple of examples of such topologies are shown together with schematic redrawings of the component filaments showing their topologies (Figure 4.4 (c) and 4.4 (d)). When changing handedness within a single bundle, one component filament must bend at certain point, as illustrated in the drawings. Observation of two circular filaments wrapping around each other provides further evidence of such change in handedness in a single bundle (Figure 4.4 (e)). There is no way topologically for two originally separate circular filaments to coil around each other

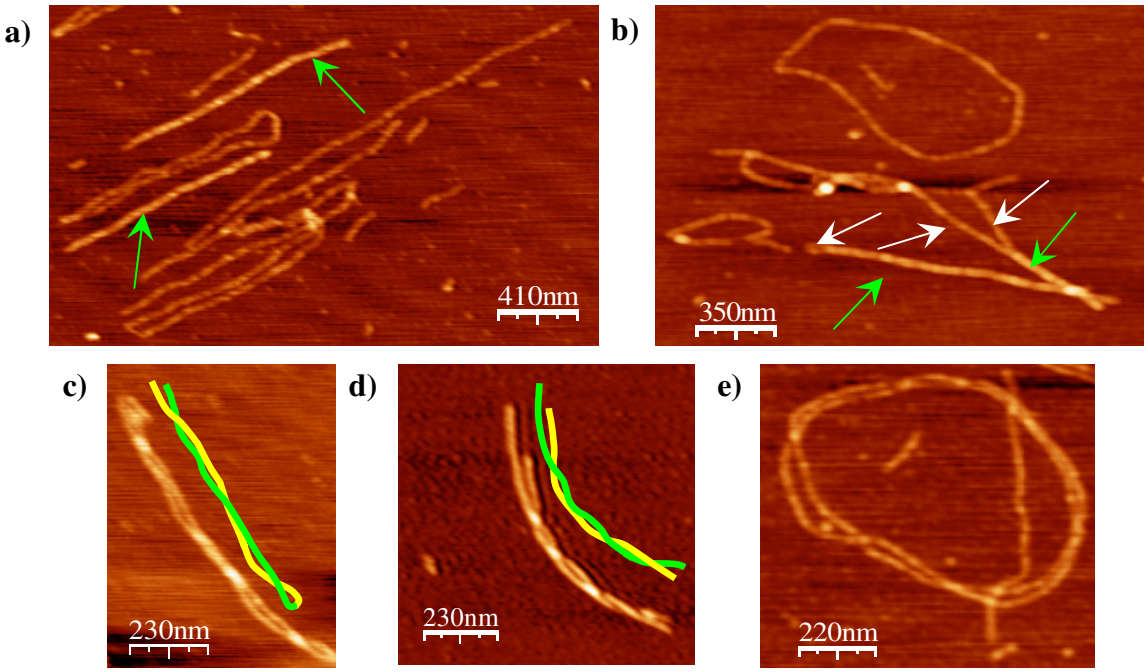

Figure 4.4. "Melted" coiling of RecA-ssDNA filaments and coexistence of both handednesses on single bundles. (a) Two completely "melted" filaments (green arrows) are otherwise hard to identify without the coexistence of non-coiled single filaments in the image; (b) The "melted" structure is confirmed in the observation that two filaments seem to "melt" into each other (green arrows) with the apparent separation of the "melted" topology into two individual filaments shown by the white arrows; (c) & (d) Coils with apparently both handednesses, in each case clarified by a schematic drawing; (e) Coiling of two circular filaments, which can only occur if both handednesses are present.

without breaking at least one of them or reversing the wrapping direction. Even though it is hard to tell the local handedness on these bundles of two circular filaments due to close wrapping, we can conclude from the presence of the wrapping of circular filaments that both handednesses are equally present in this topology. The different rigidities of RecA-ssDNA vs. RecA-dsDNA filaments might again explain the above difference between exclusive left-handedness in dsDNA filaments vs. both handednesses in ssDNA filaments since the more flexible RecA-ssDNA filaments could have more freedom to reverse their wrapping directions. The increased steric hindrance in the crowded neighborhood might contribute to the exclusive left-handedness seen on multiple-filament bundles, although further investigation is needed to explain this biased selection.

For the reason mentioned above, we did not catalogue "supercoils" of RecA-ssDNA filaments based on the number of component filaments nor analyze the pitches of "supercoils". Actually, it is hard to read the pitches of these bundles due to their close packing.

Why should ssDNA filaments occasionally "supercoil" with either handedness, while dsDNA filaments always form left-handed "supercoils"? Besides the different rigidities, another clue is the variable pitch of "supercoils" in RecA-dsDNA filaments. While we observed an average pitch of around 350 nm for RecA-dsDNA "supercoils", there were substantial variations from one "supercoil" to the next, yielding a standard deviation of around 60~80 nm, about 20% of the average pitch [14]. The variability in the pitch suggests that when filaments bind to each other, the twist in each filament might fluctuate or be altered in a non-reproducible way, influenced by the details of how the RecA units bind to each other, and the twist could be locked into a non equilibrium value,

which can be relieved by "supercoiling". Filaments of dsDNA are thought to form left-handed "supercoils" because of a non-integral number of RecA molecules per helical turn in RecA-dsDNA filaments [11]. Additional positive or negative "supercoiling" arising from the change in the pitch of individual filaments upon binding to each other could contribute to the observed variability of the left-handed "supercoiling" (positive) without changing the overall handedness of the "supercoiling". For ssDNA filaments, if there is no natural pitch of the coiling as indicated by its disordered appearance in the EM study [11], a positive or negative variation in filament pitch would lead to an overall positive or negative pitch of the coiling, which can vary from region to region within the same "supercoil". This may explain the appearance of both handednesses in two-filament RecA-ssDNA bundles, but does not explain the exclusive left-handedness observed in multi-filaments "supercoils".

Conclusions

We have found that RecA-ssDNA DNA filaments also form "supercoiled" bundles like RecA-dsDNA filament, but SSB is required since it helps loading of RecA onto ssDNA molecules. There are distinct features on these two types of bundles in terms of density of bundling and handedness. The ordered aggregation of RecA-dsDNA and the disordered aggregation of RecA-ssDNA filaments formed without SSB have been previously attributed to the non-integral number of protein units per helical turn of RecA-dsDNA filaments and the near-integral number for RecA-ssDNA filaments [11]. A later study by the same group actually shows that RecA-dsDNA and RecA-ssDNA filaments both have a non-integral number of units per turn in the presence of ATPγS [13], which

put in doubt their previous argument that "supercoiling" is the result of non-integral number of RecA proteins per helical turn of the filament. Our results clearly show that the difference in "supercoiling" is instead due at least in part to the different coverage of RecA in each DNA species. RecA can cover dsDNA molecules completely without the presence of SSB protein, but SSB protein is essential to achieve full RecA coating on ssDNA molecules. When SSB is included in the reaction, RecA-ssDNA filaments form left-handed "superhelical" bundles. The similar topology found on bundles of RecA-dsDNA and RecA-ssDNA filaments is thus a reflection of the common feature of fully-coated RecA-DNA filaments, i.e., its tendency to form "supercoils" despite that the bundles of RecA-ssDNA filaments are packaged more densely than are those of RecA-dsDNA filaments. Although it is not clear how and why these bundles are formed, a reasonable guess would be that contacts between RecA molecules on the filaments may dominate the bundling process, mediated by divalent ions such as Mg^{2+} and other factors. The difference in filament stiffness between RecA-ssDNA and RecA-dsDNA filaments is probably the cause of the different compactness of aggregates of the two filament types. The stretching modulus of RecA-dsDNA filaments (i.e., Young's modulus) has been found to be double of that of RecA-ssDNA filaments [19]. Since the bending modulus of a filament is proportional to its Young's modulus, RecA-ssDNA filaments are likely to be less resistant to collapse into densely packaged aggregates than are RecA-dsDNA filaments. For the same reason, RecA-ssDNA filaments could bend locally and shift handedness within two-filament bundles. The simultaneous coiling of multiple filaments may prevent such bending from occurring because of the strong coordination among the component filaments, but further study is needed to achieve a comprehensive

understanding of the mechanism. The existence of “supercoils” during strand exchange in the presence of ATPγS also suggests a possible role of such bundles from a biological point of view.

References

1. Kowalczykowski, S. C.; Eggleston, A. K., "Homologous pairing and DNA strand-exchange proteins", Annual Review of Biochemistry, 63991-1043 (1994)

2. M. M. Cox, Binding two DNA molecules at once: the RecA protein, in: A. Revzin (eds.), The biology of nonspecific DNA-protein interactions, CRC Press, Boca Raton, U.S.A, 1990, pp171-196.

3. Egelman, E. H., "A tale of two polymers: new insights into helical filaments", Nature Reviews Molecular Cell Biology 4, 621-630 (2003)

4. West, S. C., "Molecular views of recombination proteins and their control", Nature Reviews Molecular Cell Biology 4, 435-445 (2003)

5. Kowalczykowski, S. C.; Krupp, R. A., "Effects of Escherichia coli SSB protein on the single-stranded DNA-dependent ATPase activity of Escherichia coli RecA protein-evidence that SSB protein facilitates the binding of RecA protein to regions of secondary structure within single-stranded DNA", Journal of Molecular Biology 193, 97-113 (1987)

6. Muniyappa, K.; Williams, K.; Chase, J. W.; Radding, C. M., "Active nucleoprotein filaments of single-stranded binding protein and recA protein on single-stranded DNA have a regular repeating structure", Nucleic Acids Research 18, 3967-3973 (1990)

7. Shan, Q.; Bork, J. M.; Webb, B. L.; Inman, R. B.; Cox, M. M., "RecA protein filaments: end-dependent dissociation from ssDNA and stabilization by RecO and RecR proteins", Journal of Molecular Biology 265, 519-540 (1997)

8. Haruta, N.; Yu, X.; Yang, S. X.; Egelman, E. H.; Cox, M. M., "A DNA pairing-enhanced conformation of bacterial RecA proteins", Journal of Biological Chemistry 278 52710-52723 (2003).

9. Gonda, D. K; Radding, C. M., "The mechanism of the search for homology promoted by recA protein - facilitated diffusion within nucleoprotein networks", Journal of Biological Chemistry 261, 13087-13096 (1986).

10. Pinsince, J. M.; Griffith, J. D., "Early stages in RecA protein-catalyzed pairing - Analysis of coaggregate formation and non-homologous DNA contacts", Journal of Molecular Biology 228, 409-420 (1992)

11. Egelman, E. H.; Stasiak, A., "Structure of helical RecA-DNA complexes - II. Local conformational changes visualized in bundles of RecA-ATPγS filaments", Journal of Molecular Biology 200, 329-349 (1988)

12. Levin-Zaidman, S.; Frenkiel-Krispin, D.; Shimoni E.; Sabanay, I.; Wolf, S. G.; Minsky, A., "Ordered intracellular RecA-DNA assemblies: A potential site of in vivo RecA-mediated activities", Proceeding of the National Academy of Sciences of The United States of America 97, 6791-6796 (2000)

13. Yu, X.; Egelman, E. H., "Direct visualization of dynamics and co-operative conformational changes within RecA filaments that appear to be associated with the hydrolysis of adenosine 5′-O-(3-thiotriphosphate)", Journal of Molecular Biology 225, 193-216 (1992)

14. Shi, W. X.; Larson, R. G., "Atomic force microscopic study of aggregation of RecA-DNA nucleoprotein filaments into left-handed supercoiled bundles", Nano Letters. 5 2476-2481 (2005)

15. Sattin, B. D.; Goh, M. C., "Direct observation of the assembly of RecA/DNA complexes by atomic force microscopy", Biophysical Journal 87, 3430-3436 (2004)

16. Umemura, K.; Okada, T.; Kuroda, R., "Cooperativity and intermediate structures of single-stranded DNA binding-assisted RecA-single-stranded DNA complex formation studied by atomic force microscopy", Scanning 27, 35-43 (2005)

17. Menetski, J. P.; Bear, D. G.; Kowalczykowski, S. C., "Stable DNA Heteroduplex Formation Catalyzed by the Escherichia coli RecA Protein in the Absence of ATP Hydrolysis", Proceeding of the National Academy of Sciences of The United States of America 87, 21-25 (1990)

18. Rice, K. P.; Eggler, A. L.; Sung, P.; Cox, M. M., "DNA pairing and strand exchange by the Escherichia coli RecA and yeast Rad51 proteins without ATP hydrolysis - On the importance of not getting stuck", Journal of Molecular Biology 276, 38570-38581 (2001)

19. Hegner, M.; Smith, S. B.; Bustamante, C., "Polymerization and mechanical properties of single RecA-DNA filaments", Proceeding of the National Academy of Sciences of The United States of America 96, 10109-10114 (1999)

CHAPTER V

RECA DISSOCIATION AND ATP HYDROLYSIS HAVE DUAL ROLES DURING STRAND EXCHANGE INTERACTIONS

Chapter Summary

E. coli RecA plays an essential role in strand exchange interactions. We demonstrate that RecA dissociation exhibits a dual role during strand exchange. While it inhibits all other steps, RecA dissociation promotes completion of strand exchange by irreversibly removing RecA coating on nascent heteroduplexes, the last step in the process. The counteracting effects of RecA dissociation are evidenced by the existence of an optimal ATP regeneration level and an optimal length of incoming dsDNA at which maximum yield of nascent heteroduplexes is achieved. Because RecA dissociation is a direct effect of RecA ATPase activity, a continuous supply of ATP produced by regeneration reverses it. While a low level of ATP regeneration may limit strand exchange by deactivating RecA filaments in the early stage of strand exchange through the irreversible dissociation, a high level also inhibits the overall reaction apparently by rebinding RecA to the product DNA, thus preventing the last step of strand exchange from occurring. The effect of the length of the incoming dsDNA is also non-monotonic. This may occur because homologous recognition is faster on longer DNA molecules than on short ones, but strand switching could be slower so that the overall rate of strand

exchange is optimal at an intermediate strand length. The results also suggest the dual roles of ATP hydrolysis, i.e., deactivating active intermediates vs. propelling the strand exchange moving forward.

Introduction

The participation of RecA-like proteins in the regulation of DNA in a wide range of organisms has become evident since the discovery of RecA in *E. coli.* 30 years ago.[1-4] Despite numerous efforts to elucidate the mechanism involved in DNA strand exchange, which is the main role of RecA-like proteins, a convincingly well-established scenario that can explain thoroughly the mysterious action of RecA-like proteins is still lacking. By covering single-stranded DNA with roughly three bases per RecA monomer, RecA facilitates strand exchanges between the DNA inside a right-handed RecA-coated nucleoprotein filament and an incoming double-stranded DNA molecule with incredible efficiency. [5] RecA can also form short filaments by itself in the absence of DNA molecules provided that cofactors, such as divalent cations, ATP/ADP or their analogous, are present.[6]

The formation of complete filaments on long ssDNA by RecA requires participation of single stranded DNA binding (SSB) protein.[7-8] SSB removes secondary structures within ssDNA which otherwise impede the extension of RecA coating along the DNA after RecA nucleation. Although the presence of SSB protein also competes with RecA for the nucleation sites, it is readily removed by RecA once the growth of RecA filaments from a RecA nucleus reaches any site where SSB protein is bound.[9] Moreover, SSB protein probably assists the strand exchange interaction by binding to the

outgoing strand and thus shifting the equilibrium in the direction of strand exchange.[10] SSB might also help bypass of heterology during RuvAB mediated 3-strand and 4-strand exchange.[11]

In vitro experiments have already shown that the strand exchange interaction is a multi-step process, involving distinct intermediates, which may hard to detect due to their instability, and thus short lifetimes.[12-14] These steps include formation of nucleoprotein filaments, homologous recognition, alignment and exchange of homologous strands, displacement of the outgoing strand, and disassembly of RecA-product DNA complexes, which, taken together, constitute a very complicated, and only partially understood process. In addition, some of these steps may occur simultaneously, which makes the effort to study them individually difficult. It is commonly believed that homologous recognition is the first step.[15] This initial recognition must be fast, i.e., both homologous and heterologous dsDNA must bind quickly with the heterologous DNA unbinding quickly once the lack of homology is detected. Hence, the heterologous DNA dissociates at a rate comparable to its association, while the homologous DNA remains bound for a much longer time, allowing more complete recognition to occur. After the homology is recognized, the homologous regions of RecA-coated ssDNA and incoming dsDNA are aligned but not inter-wound, forming so-called *paranemic joint*, which requires RecA to maintain its initial structural conformation and would otherwise be unstable.[12] The paranemic joint is transformed to a *plectonemic joint* in which the incoming DNA and the invading ssDNA become inter-wound and thus such joints are stable even after dissociation of RecA protein via either ATP hydrolysis or deproteinization. Plectonemic joints are the detectable intermediates seen in most studies. Plectonemic joints may form

at the very initial contact between filaments and targeted sequences during homologous recognition, but paranemic joints are more likely to be the initial intermediates because of the lower activation energy for their formation. Finally, the outgoing strand is released from the filament and RecA dissociates from the filament, possibly simultaneously with strand release to free the nascent heteroduplexes.[16] The exchange of strands may occur either via base pair-switching or rotation of individual DNA strands, but the actual scenario still seems miraculous due to lack of direct evidence of the postulate intermediate structures (triple-stranded DNA).[17-18]

As a seemingly reversible process, the strand exchange should only depend on random diffusion, but the reverse strand exchange is only seen on short oligonucleotides using *E. coli.* RecA, not on longer DNA sequences.[19] Interestingly, there are RecA-like proteins that specifically catalyze the reverse strand exchange between a RecA-dsDNA filament and a ssDNA, but not the normal forward strand exchange.[20] The biased direction of the strand exchange catalyzed by RecA proteins may result from several factors such as ATP hydrolysis, RecA dissociation, or even SSB protein binding to the outgoing strand.

Kinetic studies show that there are at least three distinct intermediates present in the strand exchange interaction [21], making kinetic modeling of the entire scheme difficult. Actually, the process is so poorly understood at present that a simplified model with one intermediate as shown below is used in most kinetic studies.[13, 22-23] In the

$$\mathrm{Re}\,cA - SS + LDS \Leftrightarrow Intermediate \rightarrow PNDS$$

model, RecA-SS, LDS, and PNDS stand for RecA-circular ssDNA filament, linear dsDNA, and product dsDNA (nicked circular dsDNA), respectively. Pseudo rate

constants and equilibrium constants are extracted using this model. These constants are a reflection of impact from multiple factors, like ATP hydrolysis and DNA length. While their values may be roughly constant in anyone study, they vary over a wider range when results from different studies are compared. Building models with multiple steps should definitely approach more closely the actual situation, but such complex models require elaborate theories with many parameters, so enormous data sets are required to validate them, even if the model has as few as four steps.[24] We therefore approach the problem based on a complicated model, not to pursue a quantitative determination of kinetic parameters but to reach a more qualitative understanding of the kinetics. The results indicate that RecA dissociation as a direct cause of ATP hydrolysis could be the central factor that determines the efficiency of strand exchange interactions. The length of dsDNA to be exchanged also exhibits a significant effect on strand exchange as a mixed cause of different rates of ATP hydrolysis, homologous searching, and strand switching for different strand lengths.

Materials and Methods

Protein, DNA, and other reagents

Escherichia coli RecA protein, nicked circular *Φ*x174 RFII dsDNA (5386 base pairs), supercoiled *Φ*x174 RFI dsDNA, circular *Φ*x174 viron ssDNA (5386 bases), pNEB 206A dsDNA, DNA ladders, Proteinase K, 100 bp dsDNA ladder, 1k bp dsDNA ladder and six restriction enzymes (*BssH* II, *Drd* I, *Sap* I, *Bts* I, *Ssp* I, *BsoB* I) were purchased from New England Biolabs. Single stranded DNA binding protein (1–5mg/ml) was purchased from Promega. RecA protein (2mg/ml) was used as received without

further purification. ATP, ATPγS, SDS, phosphocreatine and creatine kinase were purchased from Sigma. In all preparations, molecular-biology-grade water (Eppendorf) was used and DNA was diluted with TE buffer (pH 8.0, Fisher).

Preparation of linear dsDNA fragments

Restriction fragments from 1047 bps to 5215 bps were prepared by double digestion of *Φ*x174 RFI dsDNA with *BssH* II and the other 5 restriction enzymes under manufacturer's recommended conditions, and the resulting fragments were separated by agarose gel electrophoresis at 5V/cm and collected using a Qiagen Gel extraction kit. The concentrations of these fragments were estimated by comparing their brightness with known amount of DNA ladder on a same gel using ImageJ.

Strand exchange interactions

*Φ*x174 viron ssDNA was pre-incubated with RecA protein for 10 minutes at 37 ^{o}C in the presence of phosphocreatine if ATP regeneration was used in the experiment. SSB protein and ATP or ATPγS were then added to initiate filament formation. After another 20 minutes, dsDNA fragments were introduced to initiate the strand exchange interaction. That moment is also set as the starting point of sampling. The final reaction volume is 60 μL, containing 1.4 nM viron DNA (molecular concentration), 0.56 nM dsDNA fragments, 2.65 μM RecA, 3 mM ATP (or ATPγS), and 400 nM SSB, 10 Units/mL creatine kinase and indicated amount of phosphocreatine in 1x RecA buffer (10 mM $MgCl_2$, 70 mM Tris-HCl, 5 mM Dithiothreitol, pH 7.6). The addition of phosphocreatine and creatine kinase converts ADP back to ATP, which is called ATP

regeneration. A 5μL sample was taken out at indicated intervals, subsequently deproteinized in 1% SDS and 1 mg/ml proteinase K for 30 min at 37 ^{o}C and then frozen before running on agarose gels. Samples were loaded in 0.8%~ 1.2% agarose gel and run at 5~10V/cm for 2~4hr depending on individual samples. Data were extracted from gel images by Image J.

Results and Discussion

SSB greatly enhances the yield of product DNA

As a comparison, strand exchanges with or without SSB were run in the presence with ATP (with or without ATP regeneration). Although the strand exchange can proceed to completion without the presence of SSB, the yield of the nicked dsDNA (final product) is low even with ATP regeneration (Figure 5.1, lower panel). Parallel experiments with SSB added show that the yield is greatly improved (Figure 5.1, top panel). While studies on strand exchanges between short oligonucleotides (<30 bases or bps) shows that SSB is not needed to improve efficiency [13], experiments from other groups using long DNA molecules produced results similar to ours.[17] This can be explained by low level of filament formation and inability to repel outgoing strand when SSB is absent.[7]

The effect of length of the incoming dsDNA

We have also varied the length of the incoming dsDNA so that the kinetics may be related to their lengths. It turns out that, neither the shortest (1047bps) nor the longest fragment (5215bps) produces the best yield. In stead, it is seen on the 3790-bp fragment

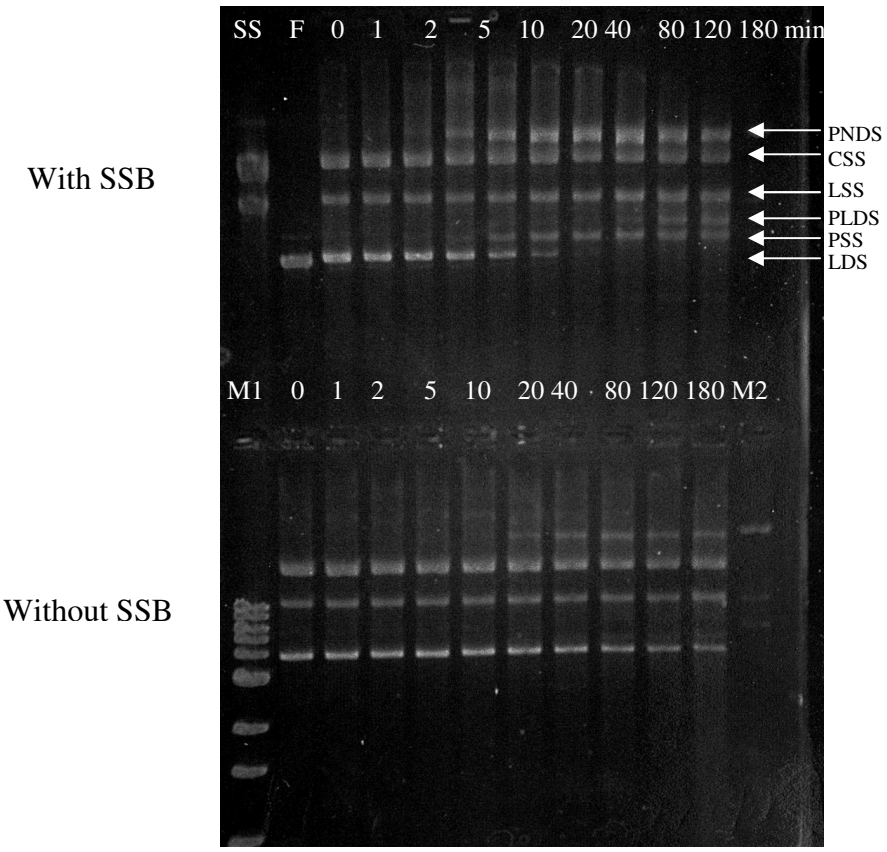

Figure 5.1. Efficiency of Strand exchange is improved in the presence of SSB. A fragment of dsDNA of 3790 bps was used in the experiment. SSB is used for the experiment shown in the top panel, but not in the lower panel. SS: original ssDNA; F: linear dsDNA fragment; M1: 1kb dsDNA Marker; M2: nicked circular phix174 RFI; CSS: original circular ssDNA; LSS: original linear ssDNA due to impurity; PLDS: product linear dsDNA; PSS: product linear ssDNA; LDS: original linear dsDNA fragment.

both with and without ATP regeneration (Figure 5.2). This unexpected dependency shows that there are some factors other than the length-related random diffusion DNA being affected by the decrease of the length of the incoming DNA which in turn change the kinetics of the strand exchange. The length of incoming DNA can at least connect with two parameters during the strand exchange, the rate of ATP hydrolysis and the efficiency of homologous searching. Binding of RecA to dsDNA (low ATPase activity) results in a decrease of rate of ATP hydrolysis compared to binding of RecA to ssDNA (high ATPase activity). [25] Therefore, ATP consumption slows down when incoming dsDNA is incorporated into RecA-ssDNA filament, and longer incoming dsDNA converts more RecA molecules bound with ssDNA to low ATPase status than shorter ones. Our parallel study on aggregation behavior of RecA-ssDNA filaments and dsDNA using ATPγS shows long DNA tends to form coaggregates faster than shorter ones. The number of individual objects seen on each image decreases both with the increase of incubation time and dsDNA length, suggesting the tendency of faster formation of larger aggregates with longer dsDNA. Since aggregation probably acts as a direct cause of efficient homologous recognition [26-27], long DNA molecules may advance short ones in term of homologous searching. But short DNA can apparently switch strand faster than longer one. The mixed effect from these aspects may explain the above result seen in this study.

The effect of ATP regeneration

As stated earlier, ATP is not required to generate strand exchange products, but the presence of ATP improves the yield a lot together with SSB. The yield is even higher

a)

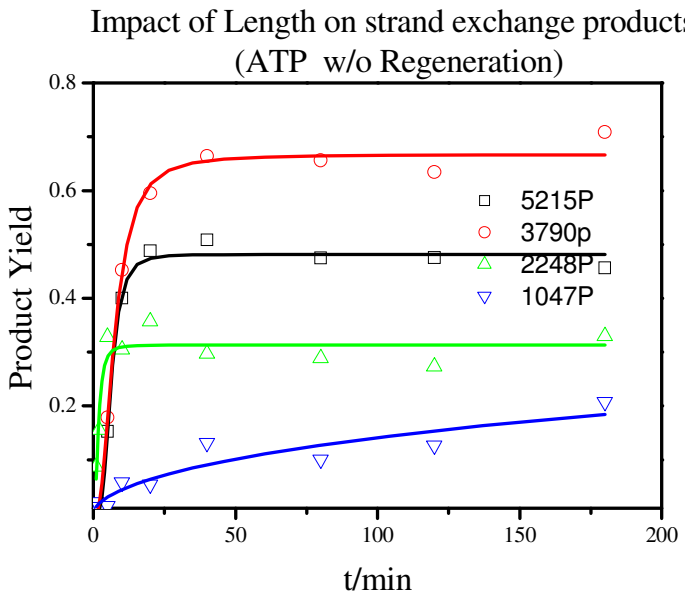

b)

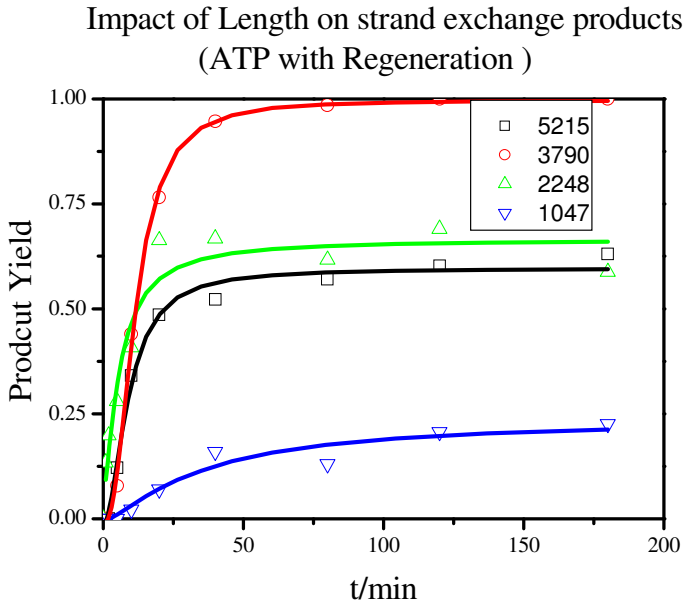

Figure 5.2. Dependency of product yield on the length of incoming dsDNA. An optimal length exists in the reaction without or with ATP regeneration. In both cases, dsDNA of 3790 bps shows much high yields than dsDNA at all other lengths, and the dsDNA of 1047 bps always have the lowest yield in a reaction period of 3hrs. Reactions were conducted (a) without ATP regeneration; (b) with ATP regeneration of 10mM phosphocreatine

.

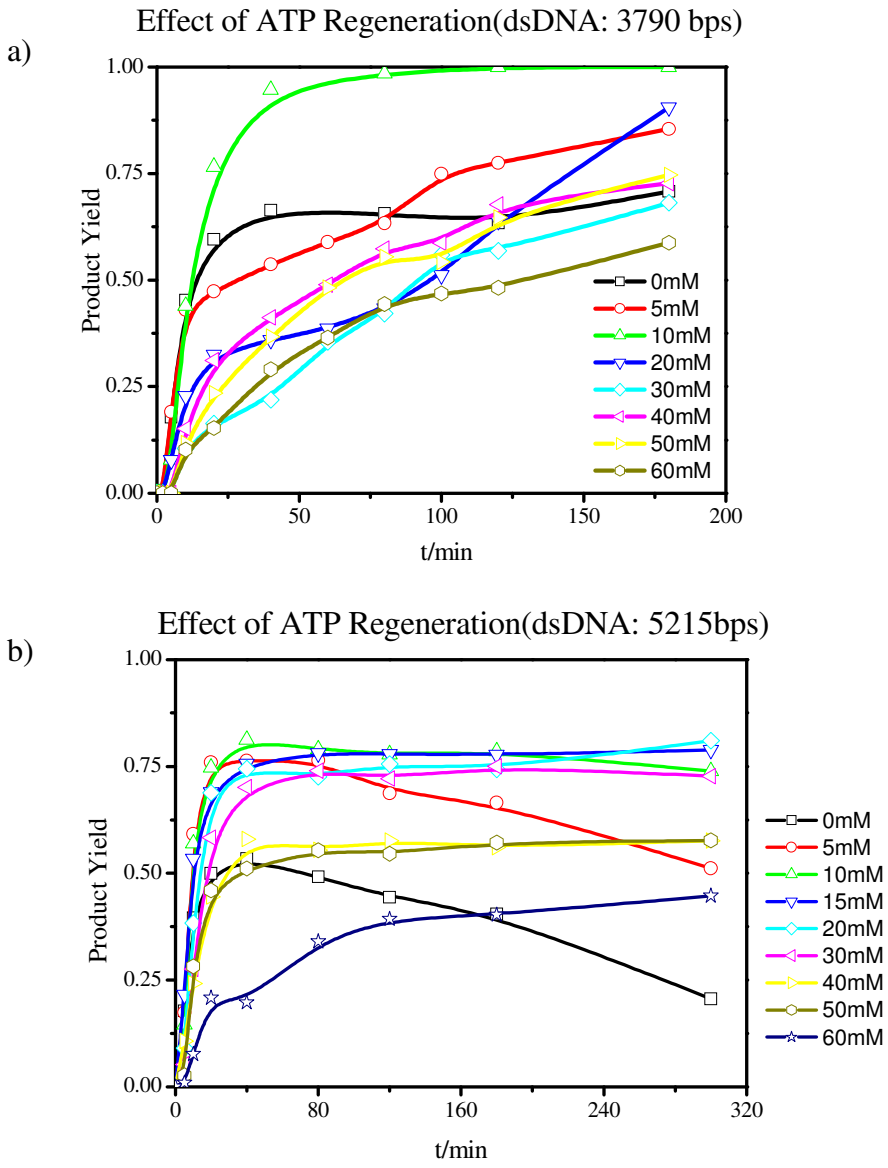

Figure 5.3. Dependency of product yield on the concentration of phosphocreatine (ATP regeneration). An optimal concentration of phosphocreatine exists during strand exchange (a) on the 3790-bp dsDNA and (b) 5215-bp DNA. In both cases, the optimal concentration of phosphocreatine is around 10mM.

a)

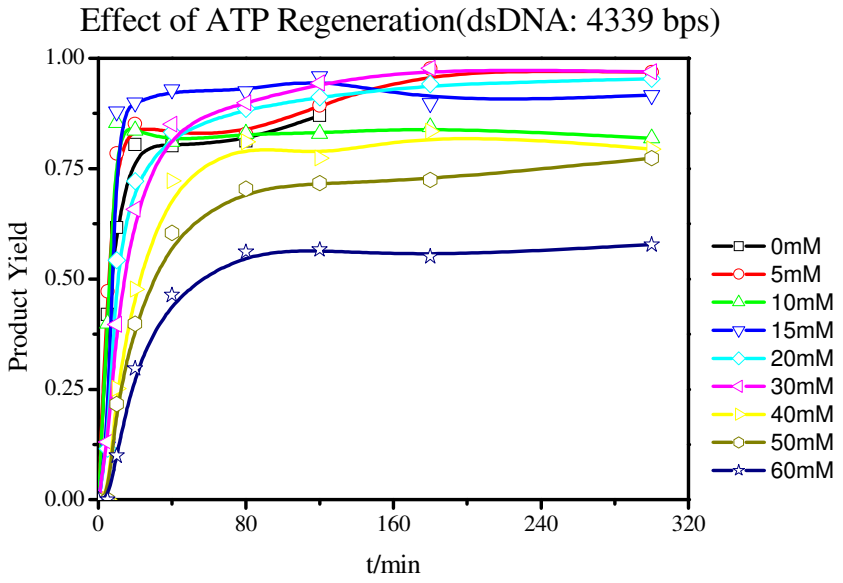

b)

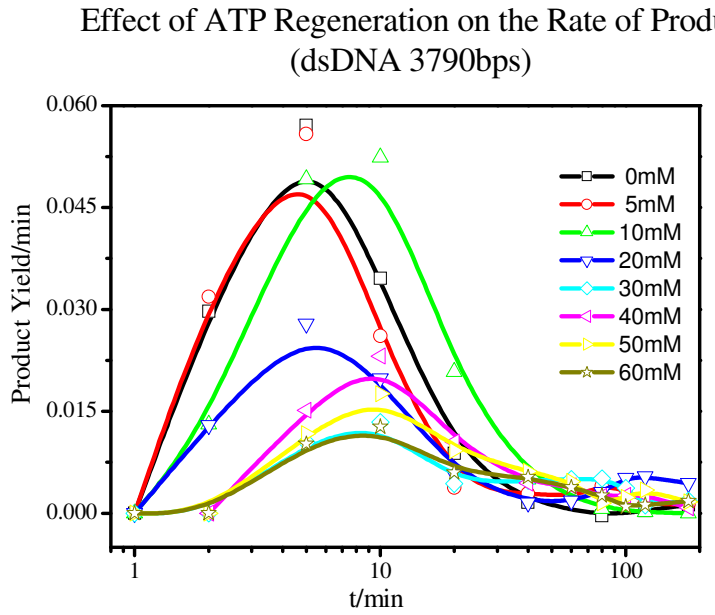

Figure 5.4. Dependency of product yield on the concentration of phosphocreatine (ATP regeneration). (a) An optimal concentration of phosphocreatine exists during strand 4339-bp dsDNA; (b) Derivative of Figure 5.3 (a) shows a time shift for rate maximum from ~5min to ~10min as the concentration of phosphocreatine increases.

when ATP is regenerated. Does this mean keeping ATP regenerated is beneficial? That is not always the case. An optimal concentration of phosphocreatine is found around 10~30mM, depending on the length of the incoming dsDNA. The product yield is maximized at the optimal concentration, and further increase in the concentration of phosphocreatine actually causes a decrease in yield as seem in Figure 5.3 (a) and (b) for 3790-bp and 5215-bp dsDNA, respectively. The similar trend is seen on a 4339-bp dsDNA as shown in Figure 5.4 (a). The trend is not apparent on short dsDNA fragments due to difficulty to separate different species with similar mobility. When the rate of yield is compared, there is an apparent shift of the appearance of rate maximum from around 5 min to 12 min during the strand exchange on the 3790-bp dsDNA as the concentration of phosphocreatine increases, clearly indicating an inhibitory effect of high-level ATP regeneration to the strand exchange (Figure 5.4 (d)). Maintaining ATP level for a long time in the system may be desired to keep the filament in its active state by preventing RecA dissociation, but it also creates a kinetic barrier for the release of the outgoing strand since RecA dissociation is one of the driven forces of this final step other than binding of SSB to the outgoing strand.

The kinetic model

A complicated kinetic model is set up and shown in Figure 5.5. In this model, there are four intermediates which contain all three strands. Both I_a and I_b are instable and decompose to original DNA species and product DNA species upon deproteinization, respectively. All species present as filaments have two statuses, active or inactive status, regulated directly by ATP hydrolysis, RecA dissociation and rebinding. Although, ATP

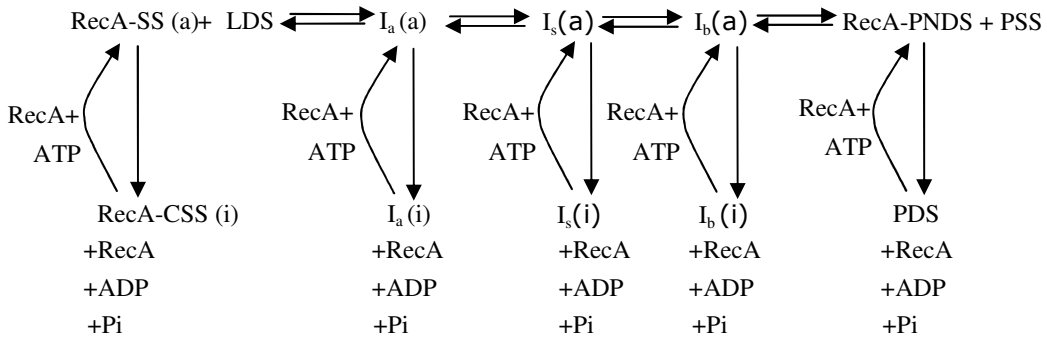

Figure 5.5. A complicated scheme of RecA mediated strand exchange showing dual roles of ATP hydrolysis and RecA dissociation. PSS: product ssDNA. All species in the reaction are constantly in a cycle of deactivation and activation, i.e., transformation between active form (a) and inactive form (i), depending on the ATP level in the reaction. While ATP hydrolysis drives the reaction forward, it also dysfunctions active species if there is no continuous supply of ATP. But keeping ATP level high also inhibits the last step in this chain reaction by binding of RecA to PNDS (reverse reaction of the last step).

hydrolysis and RecA dissociation proceed all the time, the net transition from active and inactive form does not occur until ATP level decreases to some critical level so that the reverse binding of RecA is prohibited. If ATP is continuously supplied, this dynamic reversible process drives the strand exchange all the way forward until in the last step in which the product DNA can only possibly released by continuous RecA dissociation provided that the second last step is promoted by the presence of SSB. As shown in the scheme, the rebinding of RecA in the last step is actually unwanted for driving reaction forward. Therefore, on one hand, the ATP level is expected to high enough to ensure all intermediates and the initial RecA-ssDNA filaments can stay in their active form longer enough so that the reaction initially proceeds without any inhibitory effect from the last step (There are no product DNA initially). On the other hand, this ATP level should drop and allow irreversible RecA dissociation before the accumulation of the RecA-product DNA significant inhibits the whole process. In other words, the ATP level should be optimized to meet the contradictory requirements between the first four steps and the last step over a reasonable timeframe. A too low level of ATP may allow the last step proceeding irreversibly early, but the net transformation from active to inactive form also occurs early, which inhibits the strand exchange from its early steps. Clearly, dual roles of ATP hydrolysis and RecA dissociation can be defined. In term of ATP hydrolysis, while it drives the whole strand exchange faster, it also leads to RecA dissociation and turns active species into inactive. This dual role of ATP hydrolysis is parallel in time, but that of RecA dissociation is sequential in time since the contradictory effects appear in different steps during the strand exchange. In addition, the production of RecA-PNDS is promoted by SSB since SSB could assist the release of PNDS by binding to PSS. As a

whole, SSB promotes the strand exchange in the second last step and RecA dissociation promotes the process in the last step but could inhibit all other steps

The length of the incoming dsDNA has several impacts on the kinetics of the strand exchange. First, long DNA seems to exhibit a high efficiency of homologous recognition due to the fast formation of aggregates. Although it is not clear how the homology is fast recognized in vivo, the study on the coaggregation of RecA filament and DNA indicate that such aggregation may assist homology searching by concentrating all species in a confined volume.[5] Secondly, the overall consumption rate of ATP decreases as the incoming dsDNA binding to RecA-ssDNA filament. The single molecular catalytic constant is ~30 min^{-1} when RecA binding to ssDNA, while it is only ~20 min^{-1} when RecA binding to dsDNA or dsDNA being taken into RecA-ssDNA filaments.[25] Thus, the total decrease in RecA ATPase activity is proportional to the amount of RecA being converted to the low activity status, which is determined by the length of the incoming dsDNA.

Possible problems in the experiment

Several artificial factors need to be addressed when the data from gel electrophoresis based on this model is interpreted. One is from deproteinization. Some intermediates during strand exchange are instable and may be converted to either original DNA species or product species after deproteinization. For example, the product dsDNA (PNDS) after deproteinization could at least compose of four different species which are present before deproteinization, the true product DNA, the product DNA wrapped by RecA (RecA-PNDS), I_b and I_{bI}. Dependent on the actual kinetic, the additional amount of

product DNA or original DNA due to deproteinzation could account for a large percentage of the band brightness seen in the gels, which may conceal the actual scenario. The other is the inaccuracy in determining the amount of intermediates, mostly due to the existence of intermediates in various conformations, resulting in a smeared appearance on gels. Lastly, the determination of the concentration on the dsDNA fragments after being extracted from agarose gels is probably very crude. This may put the observation of optical length of the strand exchange in doubt.

Conclusions

The kinetics during RecA-mediated strand exchange has been studied using gel electrophoresis. By changing the concentration of phosphocreatine, an optimal concentration has been identified at which the strand exchange product reaches the maximum yield. A similar trend is also found when the length of the incoming dsDNA is varied, though the result may be in doubt due to the uncertainty in the determination of the concentration of initial dsDNA after it has been extracted from agarose gels. An analysis on a complicated kinetic model indicates dual roles of ATP hydrolysis and RecA dissociation during the strand exchange interaction, which is consistent with the observation of the optimums.

References

1. Radding, C. M.; Gonda, D. K., "By searching processsively RecA Protein pairs DNA molecules that shares a limited stretch of homology", Cell 34, 647-654 (1983)

2. van Noort, J.; van der Heijden, T.; de Jager, M.; Wyman, C.; Kanaar, R.; Dekker, C., "The coiled-coil of the human Rad50 DNA repair protein contains specific segments of increased flexibility", Proceeding of the National Academy of Sciences of The United States of America 100, 7581-7586 (2003)

3. Datta, S.; Prabu, M. M.; Vaze, M. B.; Ganesh, N.; Chandra, N. R.; Muniyappa, K.; Vijayan, M., "Crystal structures of Mycobacterium tuberculosis RecA and its complex with ADP-AlF4: implications for decreased ATPase activity and molecular aggregation", Nucleic Acids Research 28, 4964-4973 (2000)

4. Hedayati, M. A.; Steffen, S. E.; Bryant, F. R., "Effect of the Streptococcus pneumoniae MmsA protein on the RecA protein-promoted three-strand exchange reaction - Implications for the mechanism of transformational recombination", Journal of Biological Chemistry 277, 24863-24869 (2002)

5. Cox, M. M., "Binding two DNA molecules at once: the RecA protein" in: Revzin A. (eds.), "The biology of nonspecific DNA-protein interactions" CRC Press, Boca Raton, U.S.A, 1990, 171-196

6. Yu, X.; Egelman, E. H.., "Structural data suggest that the active and inactive forms of the RecA filament are not simply interconvertible", Journal of Molecular Biology 227, 334-346 (1992)

7. Kowalczykowski, S. C.; Krupp, R. A., "Effects of Escherichia coli SSB protein on the single-stranded DNA-dependent ATPase activity of Escherichia coli RecA protein-evidence that SSB protein facilitates the binding of RecA protein to regions of secondary structure within single-stranded DNA", Journal of Molecular Biology 193, 97-113 (1987).

8. Muniyappa, K.; Williams, K.; Chase, J. W.; Radding, C. M., "Active nucleoprotein filaments of single-stranded binding protein and recA protein on single-stranded DNA have a regular repeating structure", Nucleic Acids Research 18, 3967-3973 (1990)

9. Joo, C.; McKinney, S. A.; Nakamura, M.; Rasnik, I.; Myong, S.; Ha, T., "Real-time observation of RecA filament dynamics with single monomer resolution", Cell 126, 515-527 (2006)

10. Haruta, N.; Yu, X.; Yang, S. X.; Egelman, E. H.; Cox, M. M., "A DNA pairing-enhanced conformation of bacterial RecA proteins", Journal of Biological Chemistry 278 52710-52723 (2003).

11. Adams, D. E.; West, S. C., " Bypass of DNA heterologies during RuvAB-mediated three- and four-strand branch migration", Journal of Molecular Biology 263, 582-596 (1996)

12. Kowalzcykowski, S. C.; Egglestson, A. K., "Homologous paring and DNA paring and DNA strand-exchange proteins", Annual Review of Biochemistry 63, 991-1043 (1994)

13. Bazemore, L. R.; Takahashi, M.; Radding, C. M., "Kinetic analysis of pairing and strand exchange catalyzed by RecA - Detection by fluorescence energy transfer", Journal of Biological Chemistry 272, 14672-14682 (1997)

14. Sagi, D.; Tlusty, T.; Stavans, J., "High fidelity of RecA-catalyzed recombination: a watchdog of genetic diversity", Nucleic Acids Research 34, 5021-5031 (2006)

15. Rao, B. J.; Chiu, S. K.; Bazemore, L. R.; Reddy, G.; Radding, C. M., "How specific is the first recognition step of homologous recombination?", Trends in Biochemical Sciences 20, 109-113 (1995)

16. Gumbs, O. H.; Shaner, S. L., "Three mechanistic steps detected by FRET after presynaptic filament formation in homologous recombination. ATP hydrolysis required for release of oligonucleotide heteroduplex product from RecA", Biochemistry 37, 11692-11706 (1998)

17. MacFarland, K. J.; Shan, Q.; Inman, R.; Cox, M. M., "RecA as a motor protein - Testing models for the role of ATP hydrolysis in DNA strand exchange", Journal of Biological Chemistry 272, 17675-17685 (1997)

18. Rao, B. J.; Radding, C. M., "Formation of base triplets by non-Watson-Crick bonds mediates homologous recognition in RecA recombination filaments", Proceeding of the National Academy of Sciences of The United States of America 91, 6161-6165 (1994)

19. Zaitsev E. N.; Kowalczykowski, S. C., **"**A novel pairing process promoted by Escherichia coli RecA protein: inverse DNA and RNA strand exchange", Genes & Development 14, 740-749 (2000)

20. Kim, J. I.; Cox, M. M., "The RecA proteins of Deinococcus radiodurans and Escherichia coli promote DNA strand exchange via inverse pathways", Proceeding of the National Academy of Sciences of The United States of America 99, 7917-7921 (2002)

21. Xiao, J.; Singleton, S. F., "Elucidating a key intermediate in homologous DNA strand exchange: Structural characterization of the RecA-triple-stranded DNA complex using fluorescence resonance energy transfer", Journal of Molecular Biology 320, 529-558 (2002)

22. Yancey-Wrona, J. E.; Camerini-Otero, R. D., " The search for DNA homology does not limit stable homologous paring promoted by RecA protein", Current Biology 5, 1149-1158 (1995)

23. Bazemore, L. R.; FoltaStogniew, E.; Takahashi, M.; Radding, C. M., "RecA tests homology at both pairing and strand exchange", Proceeding of the National Academy of Sciences of The United States of America 94, 11863-11868 (1997)

24. Xiao, J.; Lee, A. M.; Singleton, S. F., "Construction and evaluation of a kinetic scheme for RecA-mediated DNA strand exchange", Biopolymers 81, 473-496 (2006)

25. Cox, J. M.; Tsodikov, O. V.; Cox, M. M., "Organized unidirectional waves of ATP hydrolysis within a RecA filament", Plos Biology 3, 231-243 (2005)

26. Gonda, D. K.; Radding, C. M., "The mechanism of the search for homology promoted by RecA protein - facilitated diffusion within nucleoprotein networks", Journal of Biological Chemistry 261, 13087-13096 (1986).

27. Pinsince, J. M.; Griffith, J. D., "Early stages in RecA protein-catalyzed pairing - Analysis of coaggregate formation and non-homologous DNA contacts", Journal of Molecular Biology 228, 409-420 (1992)

CHAPTER VI

CONCLUSIONS AND FUTURE WORK

Conclusions

In the current work, we have used both fluorescence microscopy and atomic force microscopy to study the stretching of DNA molecules and the aggregation of RecA-DNA filaments. We also investigated the kinetics during RecA-mediated strand exchanges.

First, we studied the stretching of λDNA molecules on PMMA, PS, and PDMS surfaces using droplet evaporation, suctioning, and blowing methods. We have imaged DNA molecules stretched under different conditions and found that both suctioning and blowing have a better stretching compared with droplet evaporation. We have measured both the average length of stretched DNA molecules and the deposition density on the surfaces and observed that the impact from pH and surfaces on the stretching of DNA molecules using blowing method is not a simple reflection of the strength of hydrophobic interaction between the opened bases on DNA chains and the hydrophobic surfaces. We have successfully applied a dual-color imaging system in the study of DNAse I and DNA interactions.

Second, we have used atomic force microscopy to study the aggregation behavior of RecA-DNA filaments. We have seen regular left-handed "supercoiled" bundles of the filaments during the aggregation of RecA-dsDNA filaments. Both intra- and inter-filament bundles were seen on linear or circular filaments. The pitch collected on these

"supercoiled" filaments shows an average value around 320nm regardless of the number of component filaments within the bundles. We have also found that single strand DNA binding protein is essential for the formation of ordered bundles on RecA-ssDNA filaments. We have identified the difference between the bundles of RecA-ssDNA and RecA-dsDNA filaments. While aggregation of RecA-ssDNA may appear in densely packed structures where filaments seem to "melt" into each other, it is not seen on that of RecA-dsDNA. In addition, "supercoiling" of RecA-dsDNA shows solely the left-handedness while that of RecA-ssDNA exhibits predominant left-handedness with occasional right-handedness. The both handednesses are visible on a single bundle of Reca-ssDNA filaments. The previous explanation [1] on the "supercoiling" of RecA-dsDNA filament is apparently in doubt since contradictory arguments [2] were made by the same group. Therefore, we have suggested, instead, that the aggregation may bring additional torsional stress within the bundles which in turn forces the formation of "supercoils". The process may be dominated by RecA-RecA interactions with divalent cations assisting the interaction as a linking agent in the observation of increased number of large bundles of filaments at higher concentration of magnesium.

Gel electrophoresis has been used in understanding of the complicated kinetics during RecA-mediated strand exchange interactions. By using different lengths of dsDNA molecules and changing the capacity of ATP regeneration via adjusting the concentration of phosphocreatine, we have found that there are optimums of both the length of the incoming dsDNA molecules and the concentration of phosphocreatine. We have built the connection between the observation and a sophisticated kinetic model. It is

likely that there are dual roles of ATP hydrolysis and RecA dissociation in different steps of the multi-step strand exchange, which are reflected on the optimums seen in our study.

Proposed Future Work

The following directions are suggested based on the results and understanding we already have.

The aggregation of RecA-DNA filaments in currently study used ATPyS as the cofactor. Although the structures of filaments formed with ATPys and ATP are similar, it would be better to examine the aggregation behavior of filaments formed with ATP to confirm the existence of such ordered aggregates during the strand exchange interaction involving ATP hydrolysis. The challenge is to find a way to stabilized RecA-filaments or aggregates when ATP is used since ATP hydrolysis tends to decompose the structures.

In addition, the actual kinetics during strand exchange interactions is closely related to ATP hydrolysis. Current study does not allow monitoring either the rate of ATP hydrolysis or the absolute amount of ATP/inorganic phosphate in the solution. A sensitive protocol might be built to collect the data on ATP hydrolysis together with monitoring the progress of the strand exchange. The protocol could be done by coupling the ATP hydrolysis with other enzymatic protocols. For example, the amount of inorganic phosphate may be detected in real time by using fluorescent assays, but most commercial kits are designed to detect tiny amounts of phosphate (PiPer phosphate assay, Invitrogen). If an appropriated assay can be identified, the result would provide important information for the better understanding the dual role of ATP hydrolysis.

Alternatively, both fluorescence microscopy and atomic force microscopy may be used to study other systems of protein-DNA interactions. As a whole, these possible directions may help us to achieve better handling of either the instruments or the interested interactions and contribute further in the area.

References

1. Egelman, E. H.; Stasiak, A., "Structure of helical RecA-DNA complexes - II. Local conformational changes visualized in bundles of RecA-ATPγS filaments", Journal of Molecular Biology 200, 329-349 (1988)

2. Yu, X.; Egelman, E. H., "Direct visualization of dynamics and co-operative conformational changes within RecA filaments that appear to be associated with the hydrolysis of adenosine 5′-O-(3-thiotriphosphate)", Journal of Molecular Biology 225, 193-216 (1992)